nature climate change

Nation-wide mapping of tree-level aboveground carbon stocks in Rwanda

Maurice Mugabowindekwe [1,2] ✉, Martin Brandt [1] ✉, Jérôme Chave [3], Florian Reiner[1], David L. Skole [4], Ankit Kariryaa[1,5], Christian Igel [5], Pierre Hiernaux[6], Philippe Ciais [7], Ole Mertz [1], Xiaoye Tong[1], Sizhuo Li[1,8], Gaspard Rwanyiziri [2,9], Thaulin Dushimiyimana[1], Alain Ndoli[10], Valens Uwizeyimana [11,12], Jens-Peter Barnekow Lillesø [1], Fabian Gieseke[5,13], Compton J. Tucker[14], Sassan Saatchi[15] & Rasmus Fensholt [1]

Trees sustain livelihoods and mitigate climate change but a predominance of trees outside forests and limited resources make it difficult for many tropical countries to conduct automated nation-wide inventories. Here, we propose an approach to map the carbon stock of each individual overstory tree at the national scale of Rwanda using aerial imagery from 2008 and deep learning. We show that 72% of the mapped trees are located in farmlands and savannas and 17% in plantations, accounting for 48.6% of the national aboveground carbon stocks. Natural forests cover 11% of the total tree count and 51.4% of the national carbon stocks, with an overall carbon stock uncertainty of 16.9%. The mapping of all trees allows partitioning to any landscapes classification and is urgently needed for effective planning and monitoring of restoration activities as well as for optimization of carbon sequestration, biodiversity and economic benefits of trees.

Trees both inside and outside forests are important features of many ecosystems[1]. Individual tree traits are key determinants of ecosystem services including carbon storage, climate regulation and fuel wood[2,3]. Many countries regularly evaluate, quantify and monitor forests using field inventories as part of national forest monitoring systems[4–6]. Forest inventories are the backbone to measurement, reporting and validation (MRV) for climate change mitigation initiatives such as national level REDD+ (reducing emissions from deforestation and forest degradation)[5,6], Sustainable Development Goals (SDGs) especially SDG 15 (ref.[7]), the Paris Agreement[8] and the Bonn Challenge[9]. In many northern

countries, sample-based forest inventories are often accompanied by airborne LiDAR campaigns, providing detailed information on the carbon stocks of forests. However, field inventories and LiDAR campaigns are expensive and labour intensive[4], resulting in trade-offs between accuracy, reproducibility and the frequency of reporting. In many tropical countries, financial and human resource constraints limit the coverage and frequency of the field inventories.

This is particularly problematic for many African countries, where submetre and country-scale LiDAR data are not available across a variety of landscape types, ranging from savannas, woodlands, subhumid

[1]Department of Geosciences and Natural Resource Management, University of Copenhagen, Copenhagen, Denmark. [2]Centre for Geographic Information Systems and Remote Sensing, College of Science and Technology, University of Rwanda, Kigali, Rwanda. [3]Laboratoire Evolution et Diversité Biologique, CNRS, UPS, IRD, Université Paul Sabatier, Toulouse, France. [4]Global Observatory for Ecosystem Services, Department of Forestry, Michigan State University, East Lansing, MI, USA. [5]Department of Computer Science, University of Copenhagen, Copenhagen, Denmark. [6]Pastoralisme Conseil, Caylus, France. [7]Laboratoire des Sciences du Climat et de l'Environnement, CEA/CNRS/UVSQ/Université Paris Saclay, Gif-sur-Yvette, France. [8]Université Paris Saclay, Gif-sur-Yvette, France. [9]Department of Geography and Urban Planning, College of Science and Technology, University of Rwanda, Kigali, Rwanda. [10]International Union for Conservation of Nature—Eastern and Southern Africa Region, Kigali, Rwanda. [11]General Directorate of Land, Water, and Forestry, Ministry of Environment, Kigali, Rwanda. [12]Division of Forest, Nature and Landscape, Department of Earth and Environmental Sciences, KU Leuven, Leuven, Belgium. [13]Department of Information Systems, University of Münster, Münster, Germany. [14]Earth Sciences Division, NASA Goddard Space Flight Center, Greenbelt, MD, USA. [15]Jet Propulsion Laboratory, California Institute of Technology, Pasadena, CA, USA. ✉e-mail: mmu@ign.ku.dk; mabr@ign.ku.dk
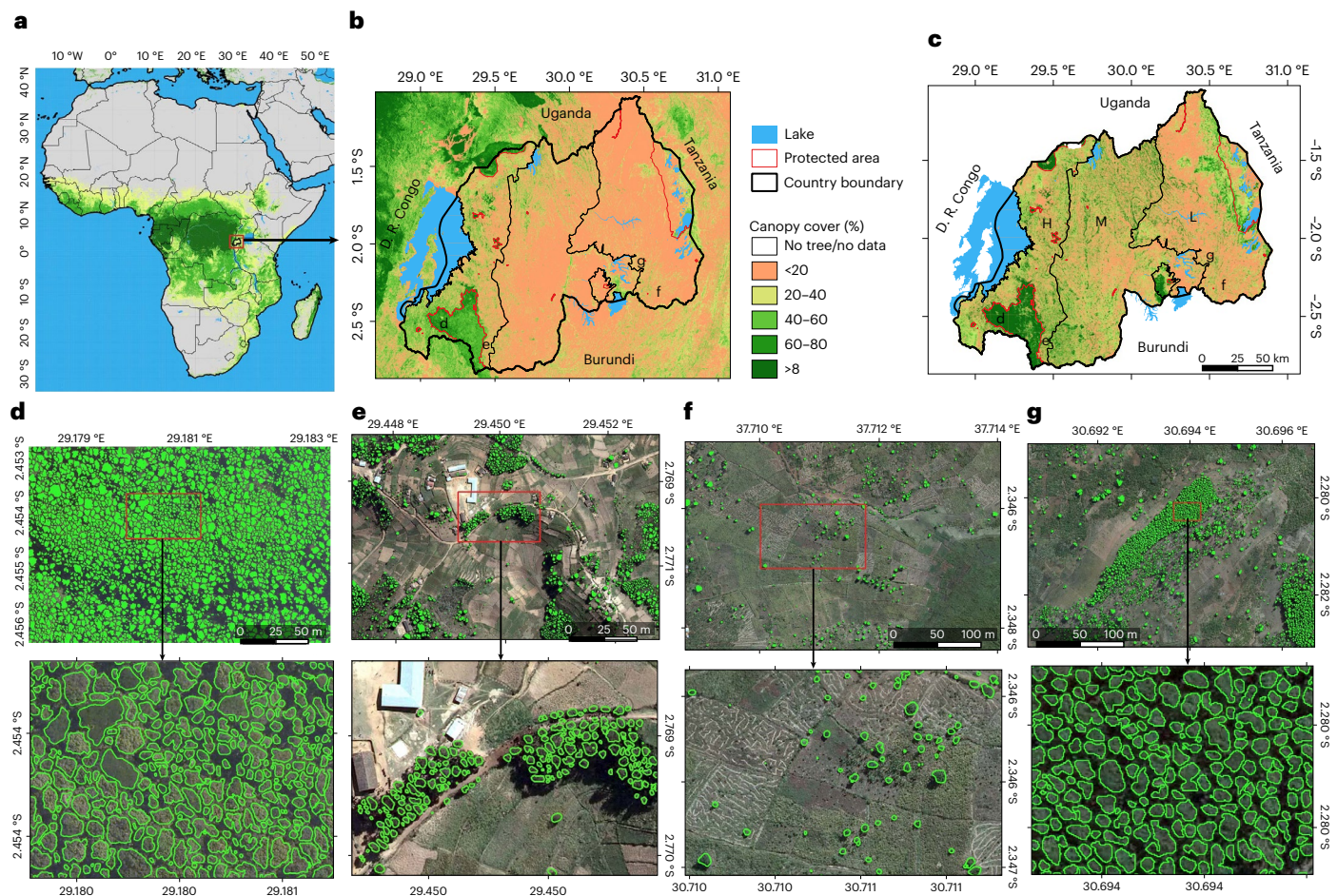
Fig. 1 | Mapping of individual trees inside and outside of forests in Rwanda.
a,**b**, Tree cover from a previously published global tree cover map using Landsat data in Africa (**a**) and in Rwanda (**b**). Global tree cover data in **a** and **b** from ref. [15]. **c**, Country-wide tree cover estimated by deep learning from 0.25 m resolution aerial imagery from 2008 (L, lowlands; M, midlands; H, highlands). Labels **d**–**g** in **a** and **b** show location of expanded panels. **d**–**g**, Examples of individual tree crown mapping in tropical montane rainforest, note that artificial gaps were filled during a postprocessing step (Methods) (**d**); *Eucalyptus* plantations (**e**); farmlands (**f**); and *Pinus* plantations (**g**). An example of previously published manual forest area delineations is shown in Extended Data Fig. 1. Boundary shapefiles of Rwanda in **b** and **c** from https://geodata.rw/portal/home/. Panel **e** adapted with permission from ref. [50], Springer Nature Limited. Credit: photographs in **d**–**g**, Swedesurvey.

and humid forests, to highly fragmented, small-scale agro-ecosystem mosaics[10,11]. This complexity makes it difficult to scale from sparsely sampled plots to the national scale. Indeed, many of these landscapes are dominated by non-forest trees which are very difficult to map with traditional methods[12,13].

Inventories and existing large-scale tree cover maps often omit an accounting of trees growing outside forests, which is related to differences in forest definitions, mapping techniques and the complexity of the environment[14–16]. This leads to incomplete censuses of trees and their related benefits and services at a national scale[17,18]. More specifically, these inaccuracies aggravate the existing uncertainties in estimates of both national carbon stocks and emission reference levels and may confound the relative contributions of emissions attributed to forest degradation or deforestation[18–20]. In turn, these inaccuracies in tree mapping complicate adequate natural resource management, climate change decision-making and policy formulation[21]. These challenges are especially notable in the tropics, where many landscape restoration projects have been initiated without fully functional monitoring systems in place[22,23].

In Africa, the rate of tree cover loss in natural forests and projected biomass losses from climate change have prompted both policy and economic initiatives for the restoration of tree-dominated landscapes[24–26]. Ongoing initiatives include the African Forest Landscape Restoration

Initiative (AFR100), with more than 30 African governments making commitments to restore at least 100 million hectares of land across the continent by 2030 (ref. [22]), the Africa Low Emissions Development Strategies[27] and the Great Green Wall initiative[28]. However, there is currently no accurate and regularly updated monitoring platform to track the progress and biophysical impact of these initiatives[22,29]. Here, we propose an approach for rapidly and accurately mapping individual trees and quantifying their carbon stocks at national scale. We also illustrate how the aforementioned challenges can be addressed with efficient new monitoring tools, using Rwanda as a demonstration. The country is a signatory to most of the above-mentioned global climate mitigation initiatives and regularly reports on their implementation. Rwanda targeted at least 30% of the country to be covered by forests by the year 2020 (ref. [30]), which was achieved in 2019 (ref. [31]) and, under the Bonn Challenge, the country has also committed to restore 81% of the country's surface area by 2030 (refs. [31,32]). Moreover, Rwanda represents a great example of a place with contrasting landscape types, the full range and variety of tree-based systems and a rich mixture of land uses: drylands dominated by savannas and pastureland, plateaus dominated by agriculture and humid highlands dominated by natural forests and protected areas, including tropical montane rainforest[33].

Recently, it was demonstrated that advanced machine learning techniques can map individual trees over large dryland areas[17].
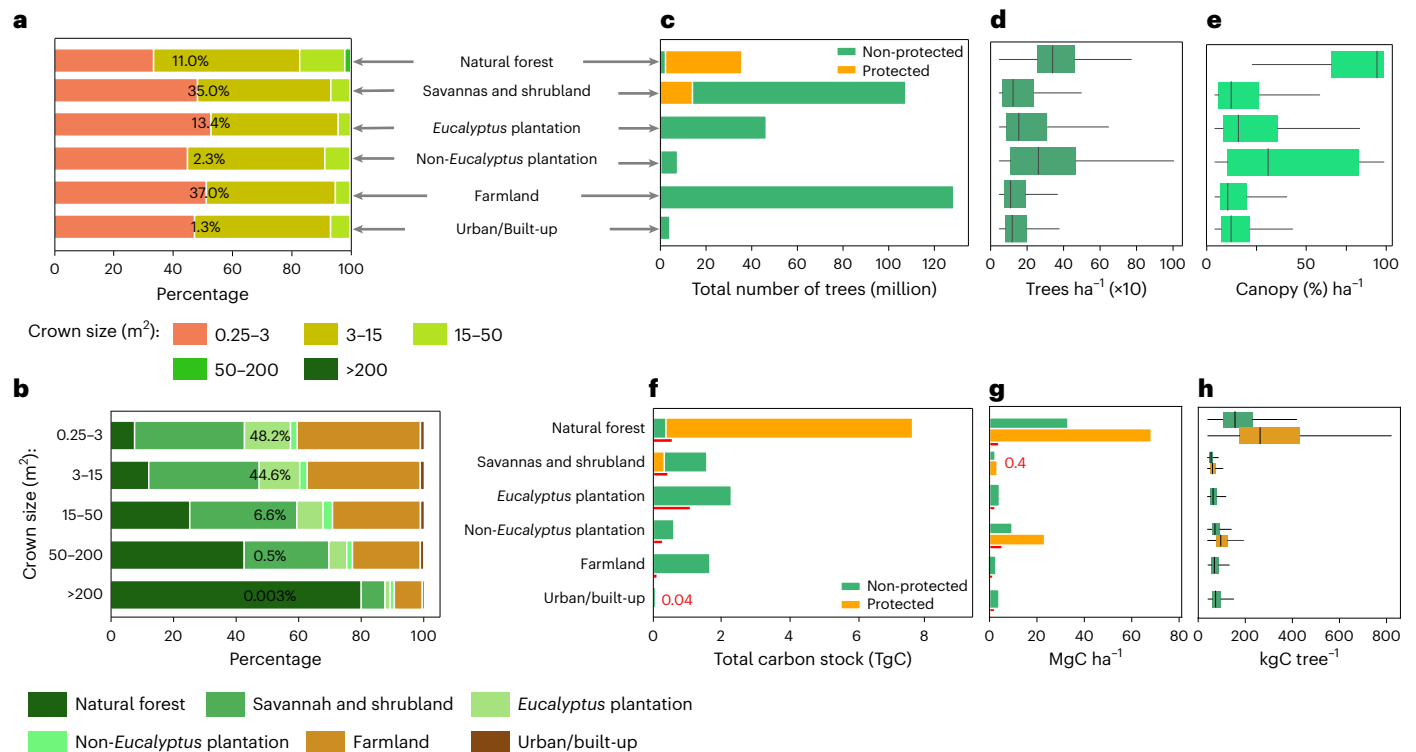
Fig. 2 | Tree counts, crown areas and carbon stocks for different land cover/use types. a, Percentage covered by different crown sizes in each land cover/use type. The percentage number shows the contribution of the land cover/use type to the total area. Crown sizes >200 m² comprise only 0.003% of the total tree count, making the class barely visible. **b**, Percentage covered by each land cover/use type in different crown size categories. **c**, Total count of trees by land cover/use. **d**, Boxplot showing the average number of trees per hectare by land cover/use type. **e**, Same as **d** but for canopy cover. **f**, Total estimated carbon stock per land cover/use type (see Methods for details on uncertainties and error propagation). **g**, Barplot showing the average carbon density per hectare per land cover/use. **h**, Boxplots showing the average carbon stock per tree per land cover/use. Number of trees = 355,268,345 (for **c–h**, *n* = 39,347,302 for natural forest; 123,381,245 for savannah and shrubland; 47,921,438 for *Eucalyptus* plantation; 8,296,494 for non-*Eucalyptus* plantation; 131,822,508 for farmland; and 4,499,358 for urban/built-up). In boxplots in **d**, **e** and **h** (from left to right), the start of the horizontal line represents the minimum value, vertical lines represent first quartile, median and third quartile values, respectively, and the end of the horizontal line represents the maximum value. The red lines in **f** and **g** are the error bars presented as absolute difference between the final carbon stock predictions and the NFI data (Extended Data Table 1). The overall uncertainty at national scale is 16.9% (Methods; Extended Data Table 1b).

However, the analysis was limited to isolated trees in savannas excluding small trees with a crown area <3 m² and did not cover other complex and heterogeneous ecosystems such as woodlands and forests. Here, we use aerial images and map both crown size and carbon stock of each individual overstory tree in Rwanda, regardless of ecosystem type. We define trees as woody plants visible from above and with a crown size of at least 0.25 m² and a visible shadow. We also show the applicability of the model trained in Rwanda in other African countries using satellite imagery. This study suggests a rapid, reproducible and highly accurate way to upscale field inventory data collected at the level of individual trees to the entire country. This will allow tree inventory reports to be of unprecedented accuracy and can support MRV of climate change mitigation initiatives.

Mapping individual trees at national scale

Aerial images with a spatial resolution of 25 × 25 cm² were acquired in 2008 covering the entire country[34] (Extended Data Fig. 1). A deep-learning model was trained using 97,574 hand-labelled tree crowns and then used to map 355,268,345 trees with crown size >0.25 m² (excluding understory). The crown area threshold was set on the basis of visual inspection of the images, as trees of this size are still clearly visible (Fig. 1). Clumped crowns were separated using a postprocessing method that determines the crown centres in the predictions, assuming that tree crowns have round shapes. The method then relabels the crown predictions on the basis of weighted distances to the identified

crown centres (Methods; Extended Data Fig. 2). Crown area and count predictions were validated with an independent test dataset and field data (Methods).

Following a manual delineation, which is based on the same aerial images as used here and which includes forest patches down to a size of 0.25 ha (ref. [35]; Extended Data Fig. 1), we stratified the landscapes into broad classes that can be found in most African countries: natural forest (including both large rainforest trees in the Nyungwe park in the southwest of Rwanda and smaller trees in the volcanoes park in the northwest), *Eucalyptus* plantations (excluding isolated *Eucalyptus* trees in farmlands), non-*Eucalyptus* tree plantations, farmlands, urban and built-up areas, as well as savannas and shrublands (Methods). We further subdivided each class in protected and non-protected areas. Overall, our results show a dominance of trees with small crown sizes of 0.25–3 m², which account for 48.2% of the mapped trees, followed by trees with crown sizes of 3–15 m², which account for 44.6% of the trees. Related to our land stratification, these two crown size ranges are dominant in farmlands and *Eucalyptus* plantations (Fig. 2a,b). Trees of the largest crown size class (crown sizes >200 m²) are very scarce and mainly found in natural forests which dominate areas under protection.

We show that only 11% of the mapped trees are located inside natural forests, whereas most trees are located in farmland (37%). Specifically, natural forests have 39.3 million trees, with a median density of 298 (s.d. 159) trees ha⁻¹ and a median canopy cover of 96.0% (s.d. 31.7). Farmlands have a median tree density of 64 (s.d. 139) trees ha⁻¹ and a
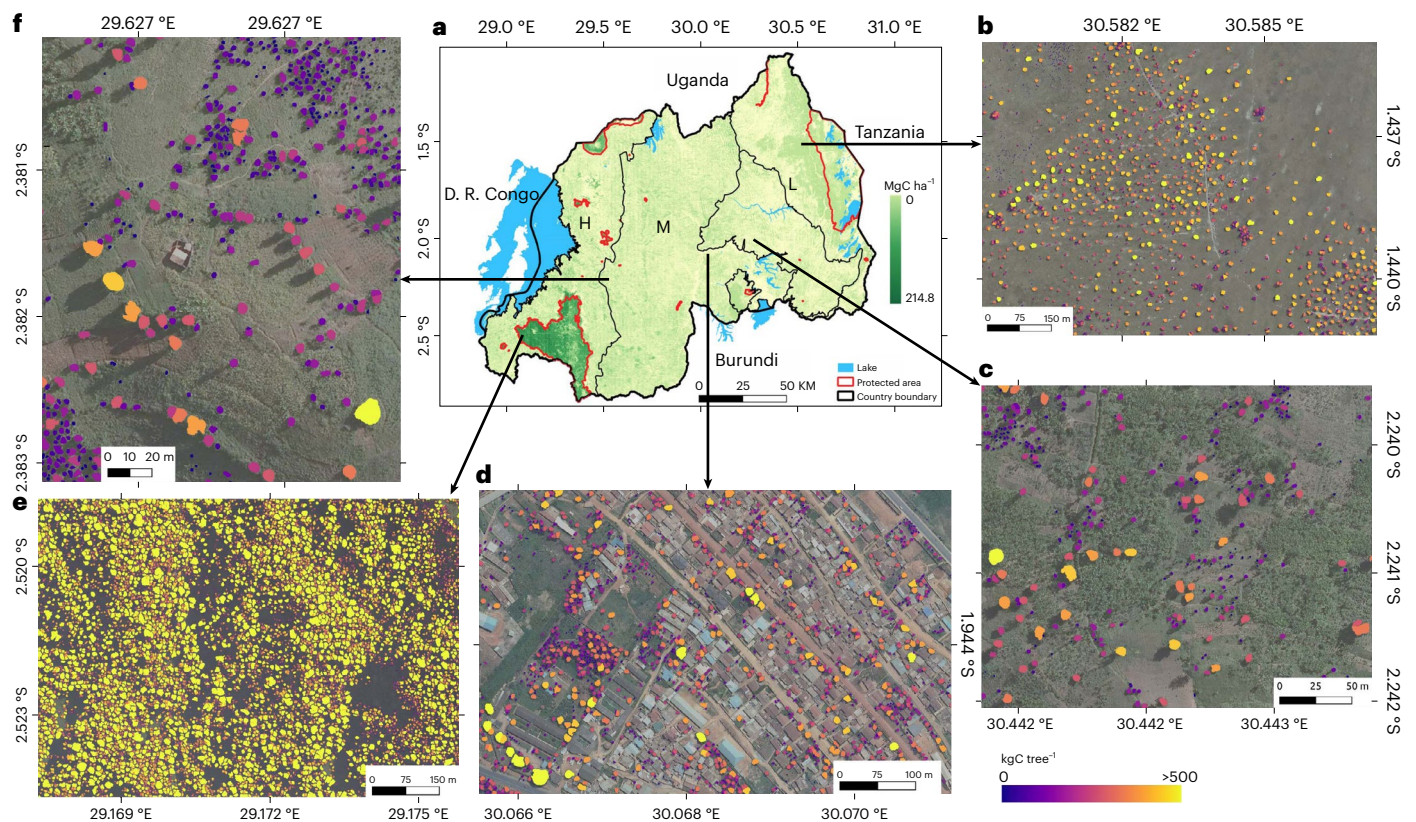
Fig. 3 | Aboveground carbon stocks at tree level in Rwanda. a, Spatial distribution of the estimated carbon stock across the major landscape types. **b–f**, Examples of estimated carbon stock per individual tree in wooded savanna (**b**), farmland (**c**), Kigali city (**d**), the tropical montane rainforest in the Nyungwe National Park (**e**) and in tree plantations (**f**). Boundary shapefiles of Rwanda in **a** from https://geodata.rw/portal/home/. Credit: photographs in **b–f**, Swedesurvey.

median canopy cover of 7.6% (s.d. 18.7). *Eucalyptus* plantations account for about 48 million trees (~13.4% of the total mapped trees), a median density of 110 (s.d. 195) trees ha^{-1} and median canopy cover of 13.9% (s.d. 26.3). Here the canopy cover is low because the manually drawn classification of plantation areas also includes bare areas close to plantations (Extended Data Fig. 1). Non-*Eucalyptus* tree plantations have 8.3 million trees (~2.3% of the total mapped trees), a median density of 221 (s.d. 222) trees ha^{-1} and a median canopy cover of 31.5% (s.d. 37.8). Urban and built-up areas have 4.5 million trees (~1.3% of the total mapped trees) and a median density of 74 (s.d. 142) trees ha^{-1}. Savannas and shrublands account for 123.3 million trees (~35% of the total mapped trees), with a median density of 100 (s.d. 164) trees ha^{-1} and a median canopy cover of 12.2% (s.d. 23.2). Overall, trees outside of natural forests are about 315.9 million trees of which 41.6% are in farmlands. The quantification of non-forest trees depends on how forests are defined. A total of 89% of the trees in Rwanda do not belong to the classes of natural forests and can thus be considered as trees outside natural forests.

The importance of protected areas for tree density and count is worthwhile to note. Although they cover only 5% of the country, they have 11% of the total mapped trees with the highest median tree density of 298 trees ha^{-1} as well as the highest median canopy cover of 96.3%. Overall, 20.8% of Rwanda was covered by trees (canopy cover) in 2008.

Carbon stocks estimated for individual trees

We used data from a field campaign in December 2021 and existing databases to estimate the stem diameter from the mapped crown sizes via allometric equations[36–39] (Methods). We then estimated the aboveground carbon stocks for each tree using existing equations based on stem diameter (Methods; Extended Data Figs. 3–5). We established land cover class-specific relationships and report here the combined results using allometric equations from ref. [38] for natural forest; ref. [39] for *Eucalyptus* and non-*Eucalyptus* plantations, farmlands and urban and built-up areas; and ref. [37] for savannas and shrublands. For each class, we evaluated the aggregated carbon stocks with data from the Rwanda National Forest Inventory (NFI) from 2013/2014 and field data from refs. [40,41], covering all land cover classes and serving as a measure of uncertainty which we quantify to 16.9% at national scale (Extended Data Tables 1 and 2). We estimate a total of 14.3 ± 2.8 Tg (± is the uncertainty) of aboveground carbon stocks in trees (Fig. 3, Extended Data Figs. 4 and 6 and Extended Data Tables 1 and 2). For areas outside the natural forests, we estimate 7.0 ± 1.1 TgC, which is 48.6% of the total national aboveground carbon stocks and slightly lower than NFI estimates (8.4 TgC). Farmlands have a total estimate of 3.5 ± 0.2 TgC corresponding to 24.4% of the national aboveground C stock with a C density of 3.0 ± 0.18 (s.d. 3.2) MgC ha^{-1}. Urban and built-up areas have 0.1 ± 0.006 TgC corresponding to 1.03% of the national aboveground C stock with a C density of 4.0 ± 0.24 (s.d. 4.0) MgC ha^{-1}. *Eucalyptus* plantations comprise a total estimate of 1.1 ± 0.6 TgC corresponding to 7.7% of the national aboveground C stocks, with a C density of 4.2 ± 2.2 (s.d. 4.3) MgC ha^{-1}. These low estimates can be explained by sparse tree planting and the regular harvesting keeping the trees young[39,40]. Non-*Eucalyptus* plantations have a total estimate of 0.3 ± 0.16 TgC corresponding to 2.2% of the national aboveground carbon stocks, with a C density of 10.0 ± 5.2 (s.d. 9.9) MgC ha^{-1}. Savannas and shrublands have 1.9 ± 0.36 TgC corresponding to 13.2% of the national aboveground C stock with a C density of 2.4 ± 0.45 (s.d. 2.4) MgC ha^{-1}. For natural forests, we estimate a median C density of 81 ± 21 MgC ha^{-1} for areas where field data are available (the Nyungwe tropical montane rainforest), which is lower than the field measurements of 121 MgC ha^{-1} (refs. [40,41]), possibly due to trees from lower layers not visible from above. Overall, we estimate that
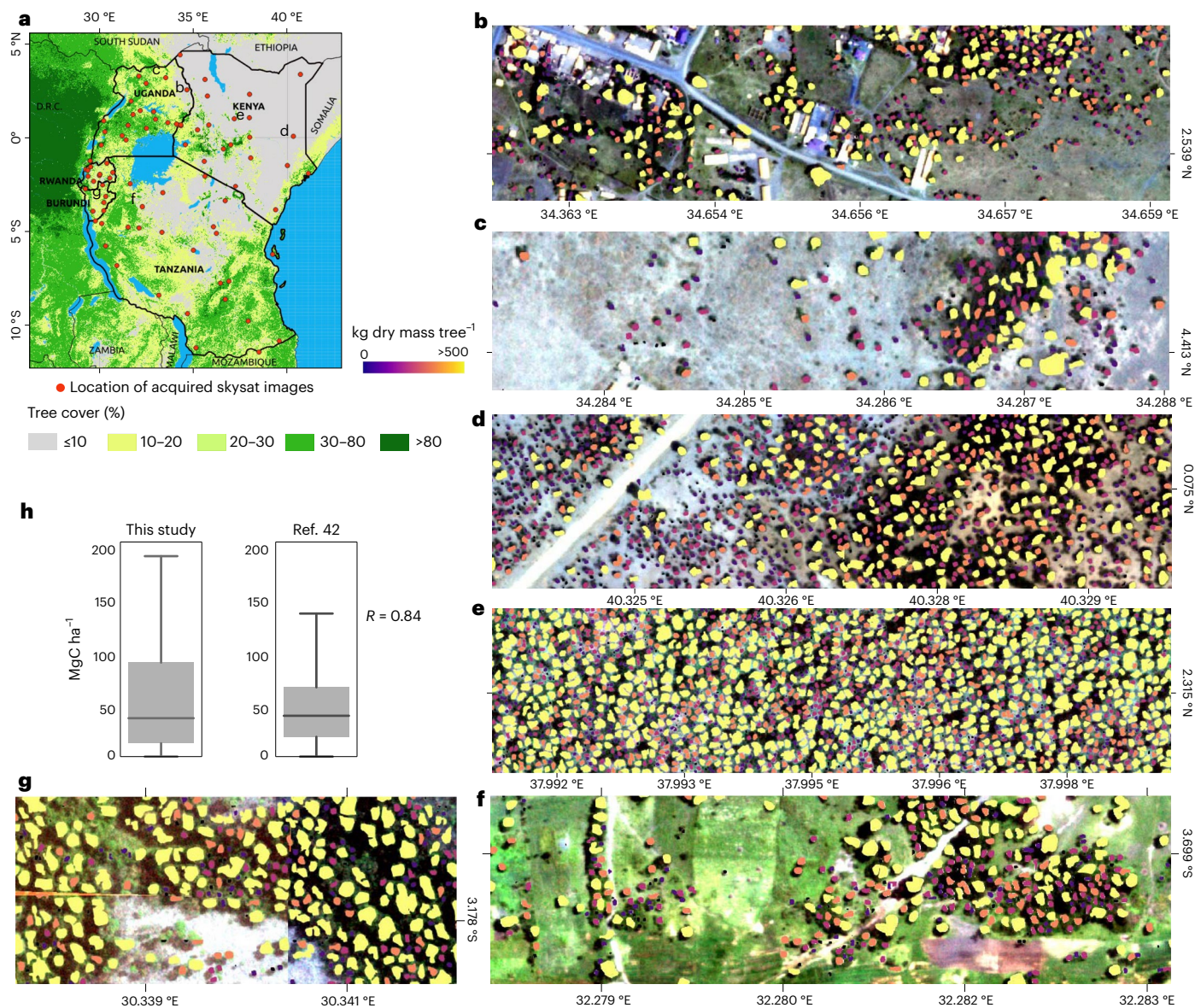
Fig. 4 | Application beyond Rwanda. a, The location of the acquired 83 Skysat images across East Africa. Tree cover data from ref. [15]. **b**–**g**, Examples of tree-level carbon stock predictions for Uganda (**b,c**), Kenya (**d,e**), Tanzania (**f**) and Burundi (**g**). **h**, A total of 150 random (n = 150) 1 × 1 km² samples were used to aggregate the predicted tree-level carbon stocks, then compare the results to a previously published map[42] using two-tailed Pearson correlation (P < 0.001). The boxplot lines from top to bottom represent the maximum, third quartile, median, first quartile and minimum values. See Extended Data Fig. 8a for more comparisons. Boundary shapefiles of East African countries in **a** from DIVA-GIS. Credit: photographs in **b**–**d**, Skysat.

51.6% of the total national aboveground carbon stocks are in natural forests with a total estimate of 7.4 ± 2.47 TgC and an overall C density of 62 ± 20 (s.d. 31.2) MgC ha⁻¹.

Scalability of the approach

We acquired 83 Skysat images at 80 cm ground sampling resolution for 2019–2021 for Tanzania, Kenya, Uganda, Burundi and Rwanda and directly applied the model trained with the aerial images from Rwanda (Fig. 4). The tree detection and crown delineation work elsewhere, even beyond Africa (Extended Data Fig. 8). We then compared the predicted carbon density from 150 randomly selected 1 × 1 km² patches with previously published maps of biomass[42–45]. Both the magnitudes of the predictions (Fig. 4b) and the spatial correlation (R = 0.84) match well with the most recent map[42].

Assessments and reporting schemes for tree resources at country scale are limited by poor data quality and ambiguous or inconsistent definitions of land cover and land use types[2,46]. Forests have been defined differently depending on location, measurement protocols and landscape contexts. When forests are specified as continuous tree cover at a predetermined mapping resolution, the underlying definition and the quality of the data product are essential to understand precisely what is being mapped and ambiguities and uncertainties result from different datasets. For instance, at medium spatial resolution >5–10 m, tree cover products may be dominated by continuous clusters of trees of a certain size and may exclude many isolated trees. Also, previous work has overestimated the extent of forests by the inclusion of shrubs and bushes as forestland[47]. Uncertainties in tree cover estimates propagate to estimations of carbon stocks, resulting in large uncertainties in biomass and carbon estimates and maps[48] (Extended Data Fig. 4 and Extended Data Table 1b).

This analysis presents an assessment of all overstory trees, aside from the assessment of their cover, density or land use. We estimate

aboveground carbon stocks at the tree level, not on an aggregate area basis as it has been in most previous carbon stock mapping. This approach is more closely aligned with standard methods and protocols for allometric scaling of carbon from inventory plots. Most allometric scaling from a tree parameter to biomass or carbon involves nonlinear relationships, where the size class distribution of trees matters for the final estimate of landscape carbon stocks. Furthermore, the ability to map all trees makes our assessment independent of forest, tree cover and land use definitions. Reporting carbon stocks on the basis of individual trees would solve important uncertainties caused by definitions, methods, data sources and spatial resolution. Our example shows that even a very detailed manual forest delineation approach missed 38.4% of the isolated trees in Rwanda, which account for 25.5% of the national aboveground carbon stocks. With results as presented here, management and conservation decision-making can be more targeted by discriminating various types of tree systems under specific conditions and in specific locations. Our approach therefore could support management of a broad array of tree-based systems such as agroforestry, as well as catalyse important cross-sector management strategies inclusive of Agriculture, Forestry and other Land Use (AFoLU). A focus on AFoLU provides a way to simultaneously manage both emission reductions and removals of greenhouse gases[49]. Integrating non-forest trees in conservation initiatives expands the scope of climate change mitigation and adaptation efforts by also accounting for trees not included in standard forest assessments[50]. Forests have been an important focal point for land cover change monitoring for decades and progress has been made developing tools and methods applied to forests[1–3]. However, less effort has been given to monitoring trees and carbon stocks for trees outside of forests. This would provide a more robust approach for reducing emissions and increasing removals, making it possible to implement comprehensive national climate change mitigation actions in countries with mostly sparse tree cover. This analysis deploys a complete inventory of trees in AFoLU as a comprehensive approach that could support a more inclusive formulation of national programmes. Moreover, when considering the large number of trees in croplands, it is possible to monitor—and thus include in policies—economically poor rural communities in marginal landscapes that are particularly vulnerable to climate change. Quantitative data as presented here have the potential to link both mitigation and adaptation in a single framework. Many of the non-forest tree systems have direct connections to livelihoods and therefore are also important for economic development, poverty alleviation and climate change resilience and adaptation. Through innovations in landscape management practices using tree-based systems and associated monitoring and reporting systems, millions of farmers could be important participants in climate change mitigation actions, while also enhancing their livelihoods at the same time. By bringing a broad array of tree-based systems into carbon monitoring platforms, there is an opportunity to increase the engagement of countries with low tree densities in climate change mitigation.

The aerial images and NFI data used here have a high quality and cover the entire country, which is a 'best-case' scenario that can hardly be met by countries with limited resources and heterogeneous landscapes. However, we have demonstrated that our model trained on aerial images in Rwanda can be directly applied on images from Skysat satellites, which can be obtained for a reasonable price for monitoring restoration projects.

We acknowledge that a satellite- or aerial image-based approach cannot resolve the full range of crown sizes because small trees are shaded out by large trees, and also the conversion of crown area to carbon stocks includes uncertainty[36] (Methods; Extended Data Table 1b). To reduce uncertainty, future versions of the proposed method should include more localized field inventory databases that allow for more local biome and species-specific wood densities and allometric conversions, as well as integrate tree height estimations from field and airborne LiDAR surveys. Ideally, national inventories are coupled with

results such as those presented here to identify systematic bias and optimize the upscaling from field plot information to country scale. If limited funds are available, low-cost imagery from PlanetScope or Sentinel-2 may be trained with tree-level data such as provided here, which would also allow a deeper temporal dimension.

Having the capability of mapping tree-level carbon stocks is important to a range of applications including monitoring of forest landscape restoration, tree plantation survival rate, forest demography: dynamics of mortality and recruitment, tree-dominated land ownership, payments for ecosystem services, issuance of concession permits and tracking compliance, among other benefits. Therefore, we emphasize the inclusion of funding for regular high-resolution imagery along with localized field inventory databases in development packages. We also highlight the relevance of all trees for conservation and protection efforts and encourage that trees outside forests are considered as equally important as trees in forests.

Online content

Any methods, additional references, Nature Portfolio reporting summaries, source data, extended data, supplementary information, acknowledgements, peer review information; details of author contributions and competing interests; and statements of data and code availability are available at https://doi.org/10.1038/s41558-022-01544-w.

References

1. Gamfeldt, L. et al. Higher levels of multiple ecosystem services are found in forests with more tree species. *Nat. Commun.* **4**, 1340 (2013).
2. Morin, X. et al. Long-term response of forest productivity to climate change is mostly driven by change in tree species composition. *Sci. Rep.* **8**, 5627 (2018).
3. Tong, X. et al. Forest management in southern China generates short term extensive carbon sequestration. *Nat. Commun.* **11**, 129 (2020).
4. Tomppo, E. et al. (eds) *National Forest Inventories Pathways for Common Reporting* (Springer, 2010).
5. *National Forest Monitoring Systems: Monitoring and Measurement, Reporting and Verification (M & MRV) in the Context of REDD+ Activities* (FAO, 2013).
6. *Voluntary Guidelines on National Forest Monitoring* (FAO, 2017).
7. *The Global Forest Goals Report 2021* (UN, 2021).
8. *Report of the Conference of the Parties on its Twenty-First Session* (UNFCCC, 2016).
9. Stanturf, J. A. et al. Implementing forest landscape restoration under the Bonn Challenge: a systematic approach. *Ann. For. Sci.* **76**, 50 (2019).
10. Naesset, E. et al. Mapping and estimating forest area and aboveground biomass in Miombo woodlands in Tanzania using data from airborne laser scanning, TanDEM-X, RapidEye, and global forest maps: a comparison of estimated precision. *Remote Sens. Environ.* **175**, 282–300 (2016).
11. Laurin, G. V. et al. Above ground biomass estimation in an African tropical forest with lidar and hyperspectral data. *ISPRS J. Photogram. Remote Sens.* **89**, 49–58 (2014).
12. Aleman, J. et al. Tree cover in Central Africa: determinants and sensitivity under contrasted scenarios of global change. *Sci. Rep.* **7**, 41393 (2017).
13. Félix, G. F. et al. Use and management of biodiversity by smallholder farmers in semi-arid West Africa. *Glob. Food Sec.* **18**, 76–85 (2018).
14. Rodríguez-Veiga, P. et al. Forest biomass retrieval approaches from earth observation in different biomes. *Int. J. Appl. Earth Obs. Geoinf.* **77**, 53–68 (2019).
15. Hansen, M. C. et al. High-resolution global maps of 21st-century forest cover change. *Science* **342**, 850–853 (2013).

16. Vancutsem, C. et al. Long-term (1990–2019) monitoring of forest cover changes in the humid tropics. *Sci. Adv.* **7**, eabe1603 (2021).

17. Brandt, M. et al. An unexpectedly large count of trees in the West African Sahara and Sahel. *Nature* **587**, 78–82 (2020).

18. Schnell, S., Kleinn, C. & Ståhl, G. Monitoring trees outside forests: a review. *Environ. Monit. Assess.* **187**, 600 (2015).

19. Mertz, O. et al. Uncertainty in establishing forest reference levels and predicting future forest-based carbon stocks for REDD+. *J. Land Use Sci.* **13**, 1–15 (2018).

20. Rinaldi, F. & Johnson, R. Accounting for uncertainty in forest management models. *For. Ecol. Manag.* **468**, 118186 (2020).

21. Gross, D. et al. Uncertainties in tree cover maps of sub-Saharan Africa and their implications for measuring progress towards CBD Aichi targets. *Remote Sens. Ecol. Conserv.* **4**, 94–112 (2018).

22. Quail, S. & Diakhite, M. *The State of AFR100: The Progress of Forest Landscape Restoration by Implementing Partners* (African Union Development Agency - NEPAD, 2022).

23. *From Reference Levels to Results Reporting: REDD+ Under the United Nations Framework Convention on Climate Change—2020 Update* (FAO, 2020); https://doi.org/10.4060/cb1635en

24. Ross, C. W. et al. Woody-biomass projections and drivers of change in sub-Saharan Africa. *Nat. Clim. Change* **11**, 449–455 (2021).

25. Hansen, A. J. et al. A policy-driven framework for conserving the best of Earth's remaining moist tropical forests. *Nat. Ecol. Evol.* **4**, 1377–1384 (2020).

26. Aleman, J. C., Jarzyna, M. A. & Staver, A. C. Forest extent and deforestation in tropical Africa since 1900. *Nat. Ecol. Evol.* **2**, 26–33 (2018).

27. Benioff, R. et al. *Low Emission Development Strategies: The Role of Networks and Knowledge Platforms* (US Department of Energy, 2013).

28. Mirzabaev, A. et al. Economic efficiency and targeting of the African Great Green Wall. *Nat. Sustain.* **5**, 17–25 (2022).

29. Niang, I. et al. in *Climate Change 2014: Impacts, Adaptation, and Vulnerability* (eds Barros, V.R. et al.) 1199–1265 (Cambridge Univ. Press, 2014).

30. *Rwanda Vision 2020—Revised in 2012* (The Republic of Rwanda, 2012).

31. *Rwanda Forest Cover Mapping* (Ministry of Environment of Rwanda, 2019).

32. Nhlapo, T. & Anderson, W. *AFR100: Toward Solutions that Protect and Restore Africa's Ecosystems and Human Well-being* (African Union Development Agency-NEPAD, 2022); https://afr100.org/content/afr100-toward-solutions-protect-and-restore-africa%E2%80%99s-ecosystems-and-human-well-being

33. Rwanyiziri, G. in *Africa Atlases. Rwanda* (eds Ben Yahmed, D. & and Houstin, N.) 86-87 (Les Éditions du Jaguar, 2013).

34. *Rwanda National Land Use and Development Master Plan—Report for Production of Orthophoto in Rwanda* (Swedesurvey, 2010).

35. Nduwamungu, J. et al. *Rwanda Forest Cover Mapping Using High Resolution Aerial Photographs* (The Global Geospatial Conference, 2013).

36. Jucker, T. et al. Allometric equations for integrating remote sensing imagery into forest monitoring programmes. *Glob. Change Biol.* **23**, 177–190.

37. Kuyah, S. et al. Allometric equations for estimating biomass in agricultural landscapes: I. Aboveground biomass. *Agric. Ecosyst. Environ.* **158**, 216–224 (2012).

38. Chave, J. et al. Improved allometric models to estimate the aboveground biomass of tropical trees. *Glob. Change Biol.* **20**, 3177–3190 (2014).

39. Mukuralinda, A., Kuyah, S. & Ruzibiza, M. Allometric equations, wood density and partitioning of aboveground biomass in the arboretum of Ruhande, Rwanda. *Trees For. People* **3**, 100050 (2021).

40. Nyirambangutse, B. et al. Carbon stocks and dynamics at different successional stages in an Afromontane tropical forest. *Biogeosciences* **14**, 1285–1303 (2017).

41. Cuni-Sanchez, A. et al. High aboveground carbon stock of African tropical montane forests. *Nature* **596**, 536–542 (2021).

42. Xu, L. et al. Changes in global terrestrial live biomass over the 21st century. *Sci. Adv.* **7**, eabe9829 (2021). https://doi.org/10.1126/sciadv.abe9829

43. Santoro, M. & Cartus, O. *ESA Biomass Climate Change Initiative (Biomass_cci): Global Datasets of Forest Above-Ground Biomass for the Years 2010, 2017 and 2018, V2* (CEDA, 2021); https://doi.org/10.5285/84403d09cef3485883158f4df2989b0c

44. Baccini, A. et al. Estimated carbon dioxide emissions from tropical deforestation improved by carbon-density maps. *Nat. Clim. Change* **2**, 182–185 (2012).

45. Bouvet, A. et al. An above-ground biomass map of African savannahs and woodlands at 25m resolution derived from ALOS PALSAR. *Remote Sens. Environ.* **206**, 156–173 (2018).

46. Castilla, G. & Hay, G. J. Uncertainties in land use data. *Hydrol. Earth Syst. Sci.* **11**, 1857–1868 (2007).

47. Bastin, J.-F. et al. The extent of forest in dryland biomes. *Science* **356**, 635–638 (2017).

48. Skole, D. L. et al. The contribution of trees outside of forests to landscape carbon and climate change mitigation in West Africa. *Forests* **12**, 1652 (2021).

49. Romijn, E. et al. Independent data for transparent monitoring of greenhouse gas emissions from the land use sector—what do stakeholders think and need. *Environ. Sci. Policy* **85**, 101–112 (2018).

50. Skole, D. L. et al. Trees outside of forests as natural climate solutions. *Nat. Clim. Change* **11**, 1013–1016 (2021).

Methods

Aerial images

We use publicly available aerial images of Rwanda at 0.25×0.25 m² resolution, collected in June–August of 2008 and 2009. The images were acquired from 3,000 m altitude above ground level, originally with a mean ground resolution of 0.22×0.22 m² pixel size then resampled to 0.25×0.25 m², using a Vexcel UltraCam-X aerial digital photography camera[34]. The images exhibit a red, green and blue band stored under 8 bit unsigned integer format. The aerial images cover 96% of the country and the remaining 4% was filled with satellite images from WorldView-2, Ikonos, Spot and QuickBird satellite sensors which are part of the publicly available dataset.

Environmental data

We use locally available climate data: mean annual rainfall, mean annual temperature and elevation data (10×10 m² resolution) to assess relationships between tree density, crown cover and environmental gradients. We also use land cover data to extract the spatial extent of plantations, forest, farmland, and urban and built-up areas for our landscape stratification. Climate data were obtained from the Rwanda Meteorological Agency as daily records from 1971 to 2017. The national forest map was manually created in 2012 using on-screen digitizing techniques over the 2008 aerial images[35]. A forest was defined as 'a group of trees higher than 7 m and a tree cover of more than 10% or trees able to reach these thresholds in situ on a land of about 0.25 ha or more'[51]. A shrub was defined as 'a group of perennial trees smaller than 7 m at maturity and a canopy cover of more than 10% on a land of about 0.25 ha or more'. The forest dataset was composed of 105,690 forest polygons, classified as either natural forest (closed natural forest, degraded natural forest, bamboo stand, wooded savanna and shrubland) or 'forest plantations' (*Eucalyptus* spp., eucalyptus; *Pinus* spp., pine; *Callitris* spp., callitris; *Cupressus* spp., cypress; *Acacia mearnsii*, black wattle; *Acacia melanoxylon*, melanoxylon; *Grevillea robusta*, grevillea; *Maesopsis eminii*, maesopsis; *Alnus acuminata*, alnus; *Jacaranda mimosifolia*, jacaranda; mixed species, mixed; and others) (Extended Data Fig. 7i). We separate shrubland from natural forest and merged it with savanna into the class 'savannas and shrublands'. We further separated tree plantations and grouped them into *Eucalyptus* and non-*Eucalyptus* plantations. Then, a farmland map was acquired from the Rwanda Land Management and Use Authority (RLMUA)[52] and overlaid with the 2012 forest cover map as a reference to clean the overlapping parts, under an assumption that the overlap is due to land use dynamics. Finally, a layer marking urban and built-up areas was acquired from RLMUA as well and the same preprocessing step as done for farmlands was applied. The combination of the land cover datasets resulted in our stratification scheme with six classes: natural forests, savannas and shrublands, *Eucalyptus* plantations, non-*Eucalyptus* plantations, farmland and urban and built-up.

Mapping of individual trees using deep learning

We used the open-source framework developed by ref. [17] to map individual tree crowns. The framework uses a deep neural network based on the U-Net architecture[53,54]. We trained the network using 97,574 manually delineated tree crowns spread over 103 areas/bounding boxes representing the full range of biogeographical conditions found across Rwanda. To cope with the challenge of separating touching tree crowns, we used a higher weight for boundary areas between crowns, as suggested in refs. [17,53]. Crown sizes in the predictions were found to be 27% smaller as compared to the manual delineations within the 103 training areas, due to the applied boundary weight that emphasizes gaps between tree crowns. Therefore, to calculate the real canopy cover, we extended each predicted tree crown by 27% and dissolved the touching crowns into continuous features. We counted single tree crowns for each hectare presented here as tree density and the percentage of each hectare covered by the extended tree crowns as canopy cover.

We developed a postprocessing method that separates clumped tree crowns and fills any gap inside a single crown (Extended Data Fig. 2). Our postprocessing method, which we refer to as detect centre and relabel (DCR), determines the crown centres in the model predictions assuming that tree crowns have a round shape and then relabels the model predictions on the basis of weighted distances to the identified crown centres. First, DCR performs a distance transform, computing for each pixel the Euclidean distance to the nearest pixel predicted as background. Let the transformed image be distance-transformed (DT). Then an $m \times m$ maximum filter is applied to DT, where m depends on the size of the smallest object to be separated. We store all pixels for which the original DT value is the same before and after max-filtering. These pixels are the instance centres as they are furthest away from the boundary and have the highest distance values within the area defined by m. In the case of several connected instance centres in regions where multiple connected pixels have the same distance from the background, only a single instance centre is kept. Finally, each pixel x predicted as a crown in the original image is assigned to its nearest instance centre, where the distance function penalizes background pixels on the connecting line between the instance centre and x.

Allometry for biomass and carbon stock estimation

Generally, allometric equations define a statistical relationship between structural properties of a tree and its biomass[55,56]. In our case, we assume a relationship between the crown area and aboveground biomass (AGB), which varies between biomes[36]. Since destructive AGB measurements are rare, we established biome-specific relationships between crown diameter (CD) derived from the crown area (CD = $2\sqrt{(\text{crown area}/\pi)}$) and stem diameter at breast height (DBH) (equations (3) and (6)). DBH has been shown to be highly correlated with AGB[36–40]. We then used established relationships from literature to derive AGB from DBH for savannas and shrublands (equation (4)), tree plantations (equation (5)) and natural forests (equation (7)). AGB was predicted for each tree and summed for 1 ha grids to derive AGB in the unit Mg per ha. Values were multiplied by 0.47 (refs. [57,58]) to derive aboveground carbon (AGC). Summed numbers over land cover classes are considered as carbon stocks. The bias as reported here was calculated following the approach from ref. [36] reporting the relative systematic error in per cent:

$$\text{bias} = \frac{1}{N}\sum_{i=1}^{N}\frac{(Y_{\text{obs}} - Y_{\text{pred}})}{Y_{\text{obs}}} \times 100 \qquad (1)$$

The error for the evaluation with NFI data was defined by:

$$\text{bias} = \frac{|\sum_N (Y_{\text{obs}} - Y_{\text{pred}})|}{|\sum_N Y_{\text{obs}}|} \qquad (2)$$

For trees outside natural forests, we used the database from ref. [36] including 10,591 field-measured trees from woodlands and savanna plus 952 samples from agroforestry landscapes in Kenya[37] to establish a linear relationship between CD and DBH (Extended Data Fig. 3a). The Kenyan dataset is compatible with the trees in Rwanda. To ensure compatibility, the Kenya data contained open-grown trees most of which are of the same families or genus as in Rwanda grown under the same conditions, the latter factor shown to be important for generalizing[37].

A major axis regression (average of four runs each 50% of the data) led to equation (3):

$$\text{DBH}_{\text{predicted}} \text{ in cm} = -4.665 + 5.102 \times \text{CD} \qquad (3)$$

Equation (3) showed a reasonable performance with a very low bias (average of four runs on the 50% not used to establish the equation (3)): $r^2 = 0.71$; slope = 0.95; root mean square error (RMSE) = 6.2 cm; relative RMSE (rRMSE) = 42%; bias = 1%). We tested equation (3) on an independent

dataset from Kenya consisting of 93 trees where AGB was destructively measured (Fig. 3b). The Kenyan database provides an uncommon opportunity to use destructive samples in which the carbon mass is not estimated indirectly and the relationship between crown area and carbon is direct: we do not need to invoke a second allometry to derive the dependent variable. All trees were open-grown trees in the same growing conditions as the agricultural areas of Rwanda. On these 93 trees, DBH can be predicted reasonably well from CD using equation (3) (r^2 = 0.84; slope = 0.86; RMSE = 8 cm; rRMSE = 25%; bias = 6%). We then applied an allometric equation from literature[37] established for non-forest trees in East Africa to estimate AGB from DBH$_{predicted}$ and compared the predicted AGB with the destructively measured AGB (r^2 = 0.81; RMSE = 511 kg; rRMSE = 55%; bias = 25%) showing an acceptable performance (Extended Data Fig. 3c) but indicating a systematic bias, which will be further tested with biome-specific field data (next section). We apply equation (4) to estimate AGB for trees outside forests in Rwanda in savannas and shrublands:

$$AGB_{predicted} \text{ in kg} = 0.091 \times DBH_{predicted}^{2.472} \tag{4}$$

Given the different structure of trees in farmlands, urban and built-up areas and plantations as compared to trees in natural forests and in natural non-forest areas, we used a different equation for trees in these areas. It was established in Rwanda using destructive samples from tree plantations[39]:

$$AGB_{predicted} \text{ in kg} = 0.202 \times DBH_{predicted}^{2.447} \tag{5}$$

A different CD–DBH relationship was established for natural forests. Here, we conducted a field campaign in December 2021 sampling 793 overstory trees in Rwanda's protected natural forest. We measured both CD and DBH and established a logarithmic major axis regression model with a Baskerville correction[59] between the two variables to predict DBH from CD (Extended Data Fig. 3d). We did four runs each using 50% of the data to establish equation (6) (average of the four runs) and the other 50% to test the performance also averaged over the four runs (r^2 = 0.71; slope = 0.99; RMSE = 13 cm; rRMSE = 45%; bias = 19%). Note that CD is extended by 27% to account for underestimations of touching crowns in dense forests (see previous section):

$$DBH_{predicted} \text{ in cm} = (\exp(1.154 + 1.248 \times \ln(CD \times 1.27)) \\ \times (\exp(0.3315^2/2))) \tag{6}$$

We then used a state-of-the-art allometric equation established for tropical forests[38] to predict AGB from DBH for natural forests in Rwanda:

$$AGB_{predicted} \text{ in kg} = \exp\left[1.803 - 0.976E + 0.976\ln(\rho) \\ + 2.673\ln(DBH) - 0.0299[\ln(DBH)]^2\right] \tag{7}$$

where E measures the environmental stress[38] (a gridded layer is accessible via https://chave.ups-tlse.fr/pantropical_allometry.htm) and ρ is the wood density. Here, we used a fixed number (0.54), which is the average wood density for 6,161 trees from ref. [40], weighted according to the abundance of the species in the plots. The relative error was calculated by the quadratic mean of the intraplot and interplot variations, which is 18.2% (Extended Data Table 1b). No destructive AGB measurements were found that showed a similar CD–DBH relationship as we measured during the field trip in Rwanda's forest. We could thus not evaluate the performance for natural forests at tree level but had to rely on plot-level comparisons (next section).

Evaluation and uncertainties of the allometry

Biomass estimations without direct measurements of height or DBH inevitably include a relatively high level of uncertainty at tree level[38,60].

Uncertainty does not only originate from the CD to DBH conversion but also the equation converting DBH to AGB. As shown in the previous section, no strong systematic bias could be detected for the CD to DBH conversion but the evaluation of the CD-based AGB prediction with an independent dataset from destructively measured AGB revealed a bias of 25%. However, this comparison (Extended Data Fig. 3c) may not be representative for an entire country having a variety of landscapes and tree species, so a systematic propagation is unlikely. We also did not have sufficient field data to evaluate the conversions in natural forests. Here, we used data from 15 natural forest plots with 6,161 trees published by ref. [40] and ref. [41] and directly compared the summed biomass of the trees we predicted over their plots. The median measured biomass for the plots is 121 MgC ha^{-1} and we predict a median biomass of 81 MgC ha^{-1} (plot-based rRMSE = 54%; bias = 11%; bias on summed plots = 26%). The overall underestimation by our prediction is not necessarily a model bias but may be partly explained by the contribution of the understory trees, which cannot be captured by aerial images. Interestingly, our C stock estimates are in the same range of magnitude as global biomass products[43–45,61] (Extended Data Fig. 4), indicating that overstory tree-level carbon stock assessments are possible from optical very high resolution images, even in tropical forests. Several global products overestimated biomass for non-forest areas like savannas or croplands, which is probably because they are calibrated in denser forests. The most recent products of ref. [42] and ref. [61] are much closer to the estimates from our results and the NFI. This is also seen in the grid-based correlation matrix where ref. [42] correlates best with our map, followed by ref. [61].

We further use NFI data from 2014 to measure the uncertainty of the final carbon stock estimates and evaluate if systematic differences between AGB predictions and field assessments can be found for different land cover classes (Extended Data Table 1). For the NFI data, a total of 373 plots with 2,415 trees were measured and species-specific allometric equations applied[62]. To identify systematic errors at landscape scale, we extracted averaged values for areas around the plots from our predictions and calculated statistics on averages over all plots. Interestingly, our predictions for farmlands only show a bias of 5.9%: we estimate on average 2.46 MgC ha^{-1} and the inventories measure 2.37 MgC ha^{-1} on their 150 plots. For savanna and shrublands, we estimate 4.16 MgC ha^{-1} while inventories measure 3.31 MgC ha^{-1} (bias = 18.9%). For plantations, we estimate lower values (8.16 compared to 16.79 MgC ha^{-1}; bias = 52.6%). To calculate the total uncertainty on country-wide C stock estimates, we weighted the bias from the different classes according to their relative area. We estimate a total uncertainty on the carbon stock predictions of 16.9% at the national scale (Extended Data Table 1).

We found a very low bias for estimated C density in farmlands (5.9% bias) which make up most of the areas outside natural forests in Rwanda (Extended Data Table 1, Extended Data Fig. 6). The high bias for plantations can be explained by three factors: large bare areas considered part of plantations by the manual delineation of plantation areas (Extended Data Fig. 1); regular harvesting and continual thinning which keep many plantation trees young and small; and the fact that our aerial images are from 2008 while plantation trees have grown until 2014 with a few new NFI plots initiated after 2008. The bias in savannas and shrublands can be explained by the following factors: the presence of multistemed trees with large crowns such as *Acacia* spp. and *Ficus* spp. among others; the fact that a crown-based method overestimates C stocks of shrubs with a small height; and presence of shrub trees with both small height and small (multiple) stems. If tree-level based carbon stock assessments derived from crown diameter as presented here should become standard to complement national inventories, a database with sufficient samples to evaluate for systematic errors needs to be established for each biome and inventory and satellite/aerial image-based methods need to be further harmonized.

To further quantify the error propagation of the CD to DBH conversion for our application, we established four equations each randomly

using 50% of the dataset and predicted the carbon stock for each tree in Rwanda with each equation. We did this separately for natural forests and trees outside natural forests. We calculated the rRMSE between the aggregated carbon stocks for each hectare. We averaged the rRMSE for each land cover class and show that the uncertainty for all classes does not exceed 5% (Extended Data Table 2a).

Evaluation and uncertainties of tree crown mapping

We created an independent test dataset, which was never seen during training and was also not used to optimize hyperparameters. The test set consists of 6,591 manually labelled trees located in 15 random 1 ha plots (Extended Data Fig. 5). Thanks to the size of the country, the plots represent all rainfall zones and three major landscapes of the country. The plot-level comparison yielded very high correlations between the predictions and the labels and is shown in Extended Data Fig. 5. We also calculated a confusion matrix showing an overall per pixel accuracy of 96.2%, a true positive rate of 79.6% and a false positive rate of 6.8% (Extended Data Table 2b). Trees outside natural forests are easy to spot and count for the human eye, so we have confidence in the plot-based evaluation. However, it is often challenging in natural forests. Here, we used again the field measurements from 15 plots with 6,161 trees[40,41]. We find that we underestimate the total tree count by 22.6%, which may, at least partly, be explained by understory trees hidden by overstory trees and which are, therefore, not visible in our images. New field campaigns are needed to better understand and calibrate our results and possibly correct for systematic bias.

Application and evaluation beyond Rwanda

We acquired 83 Skysat scenes at 80 cm for Tanzania, Burundi, Uganda, Rwanda and Kenya. The model trained on the 25 cm resolution aerial images of Rwanda from 2008 was directly applied on the Skysat images. Forest and non-forest areas were manually delineated to decide which allometric equation to use for the carbon stock conversion. We randomly selected 150 1×1 km^2 patches and aggregated the predicted carbon density per patch and compared the results with previously published maps[42–45]. Results show that the model can directly be applied to comparable landscapes on different datasets. Note, however, that accurate carbon stock predictions need local adjustments with field data. We then tested the tree crown model transferability on aerial images from California (NAIP; 60 cm) and France (20 cm) and found that the model delivers realistic results without any local training or calibration (Extended Data Figure 8).

Reporting summary

Further information on research design is available in the Nature Portfolio Reporting Summary linked to this article.

Data availability

Global tree cover maps are available at http://earthenginepartners.appspot.com/science-2013-global-forest. Climate data are freely accessible through an online application to the Rwanda Meteorological Agency via http://mis.meteorwanda.gov.rw/. Aerial images and land use and land cover data are freely available for research through formal application to the Rwanda Land Management and Use Authority at https://www.rlma.rw. Products produced in this study: tree density, tree cover, carbon stock estimates are freely accessible at https://doi.org/10.5281/zenodo.7118176 (ref. [63]). The global database with tree measurements including biomass is available from J.C. Tree measurements from Kenya are available from D.S. Tree measurements from Rwanda are available from M.M.

Code availability

The code for the tree detection framework based on U-Net is publicly available at https://doi.org/10.5281/zenodo.3978185. Support and more information are available from A.K. (ak@di.ku.dk or ankit.ky@gmail.com) or F.R. (flr@ign.ku.dk).

References

51. *Rwanda Forest Cover Mapping using High Resolution Aerial Photographs* (CGIS, 2012).
52. *Presidential Order Establishing the National Land Use and Development Master Plan, No. 058/01 of 23/04/2021* (Republic of Rwanda, 2021).
53. Ronneberger, O. et al. U-Net: convolutional networks for biomedical image segmentation. In *Proc. International Conf. on Medical Image Computing and Computer-Assisted Intervention* 234–241 (Springer, 2015).
54. Koch, T. et al. Accurate segmentation of dental panoramic radiographs with U-Nets. In *Proc. IEEE International Symposium on Biomedical Imaging (ISBI)* (eds Davis, L. et al.) 15–19 (IEEE Computer Society, 2019). https://doi.org/10.1109/ISBI.2019.8759563
55. Brown, S., Gillespie, A. J. R. & Lugo, A. E. Biomass estimation methods for tropical forests and the application to forest inventory data. *For. Sci.* **35**, 881–902 (1989).
56. Chave, J. et al. Tree allometry and improved estimation of carbon stocks and balance in tropical forests. *Oecologia* **145**, 87–99 (2005).
57. *IPCC Guidelines for National Greenhouse Gas Inventories* (IPCC, 2006).
58. Martin, A. R., Doraisami, M. & Thomas, S. C. Global patterns in wood carbon concentration across the world's trees and forests. *Nat. Geosci.* **11**, 915–920 (2018).
59. Baskerville, G. L. Use of logarithmic regression in the estimation of plant biomass. *Can. J. For. Res.* **2**, 49–53 (1972).
60. Djomo, A. N. & Chimi, C. D. Tree allometric equations for estimation of above, below and total biomass in a tropical moist forest: case study with application to remote sensing. *For. Ecol. Manag.* **381**, 184–193 (2017).
61. Hanan, N.P., Prihodko, L., Ross, C.W., Bucini, G. & Tredennick, A.T. *Gridded Estimates of Woody Cover and Biomass across Sub-Saharan Africa, 2000–2004* (ORNL DAAC, 2020); https://doi.org/10.3334/ORNLDAAC/1777
62. *Execution of a National Forest Inventor—Technical Report No. 8: Detailed Results Monitoring System for Forests and Measuring Tree Growth* (Rwanda Natural Resources Authority, 2016).
63. Mugabowindekwe, M. et al. Dataset: Nation-wide mapping of tree-level aboveground carbon stocks in Rwanda. *Zenodo* https://doi.org/10.5281/zenodo.7118176 (2022).
64. Chave, J. et al. Towards a worldwide wood economics spectrum. Ecol. Lett. 12, 351–366 (2009).
65. Hazel, D. & Bardon, R. Conversion Factors for Bioenergy—NC Woody Biomass (Oak Ridge National Laboratory, 2008); https://content.ces.ncsu.edu/conversion-factors-for-bioenergy

Author contributions

Competing interests

The authors declare no competing interests.

Additional information

Extended data is available for this paper at https://doi.org/10.1038/s41558-022-01544-w.

Supplementary information The online version contains supplementary material available at https://doi.org/10.1038/s41558-022-01544-w.

Correspondence and requests for materials should be addressed to Maurice Mugabowindekwe or Martin Brandt.

Peer review information *Nature Climate Change* thanks Julius Anchang, Christopher Ross and the other, anonymous, reviewer(s) for their contribution to the peer review of this work.

**Reprints and permissions information** is available at www.nature.com/reprints.
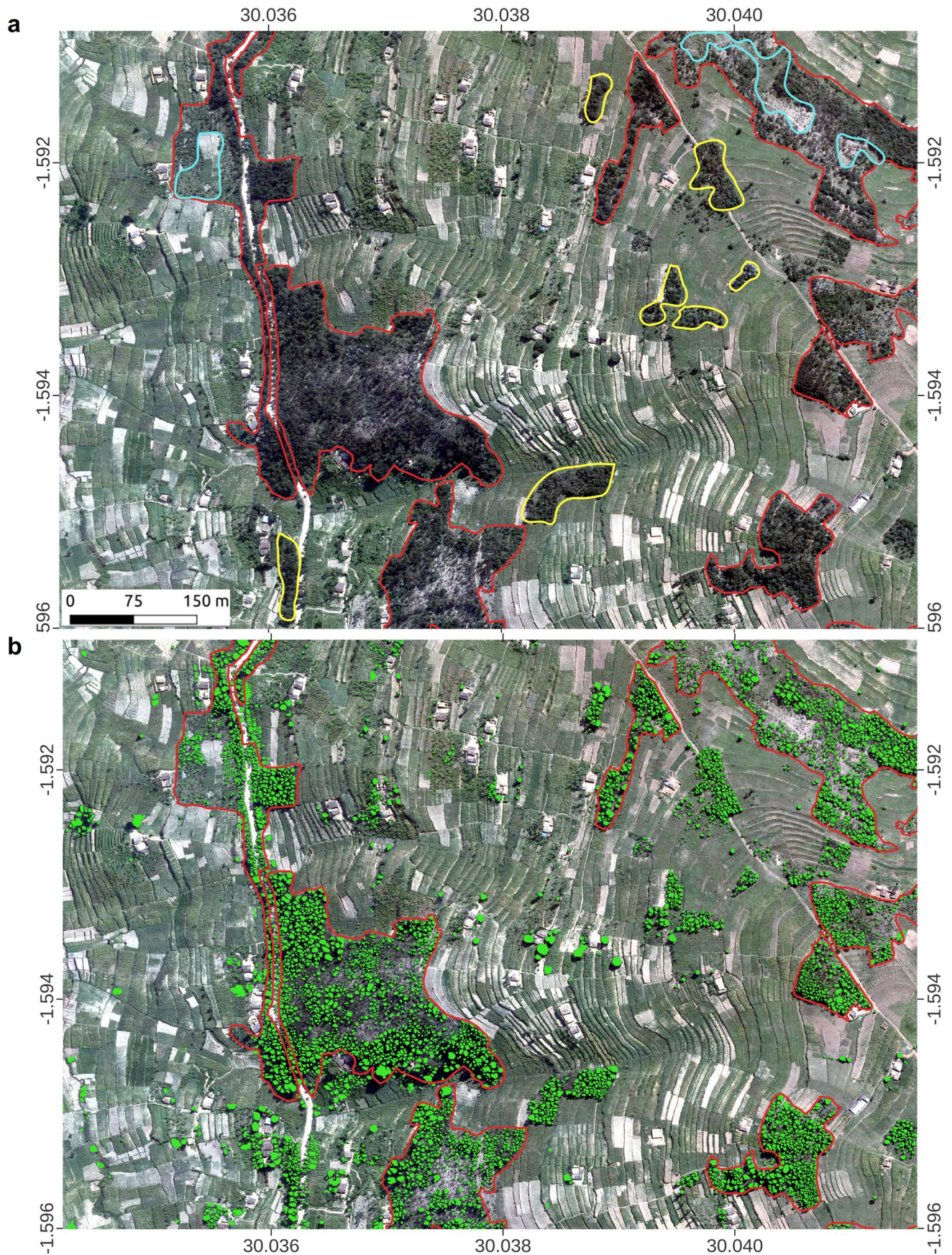
Extended Data Fig. 1 | An example showing previous manual forest delineations. The red lines are manually labelled forest boundaries from the Rwanda national forest map of 2012 (ref. [35]). **a**, Several patches which would qualify for the used forest definition were missed by the manual delineation (yellow lines). Also, some bare areas inside forest patches (cyan line) were considered as part of forests. **b**, Our results are shown in green, highlighting the improvements over the previous method. Shapefiles for national forest cover map from RFA. Credit: background photographs, Swedesurvey.

a

b
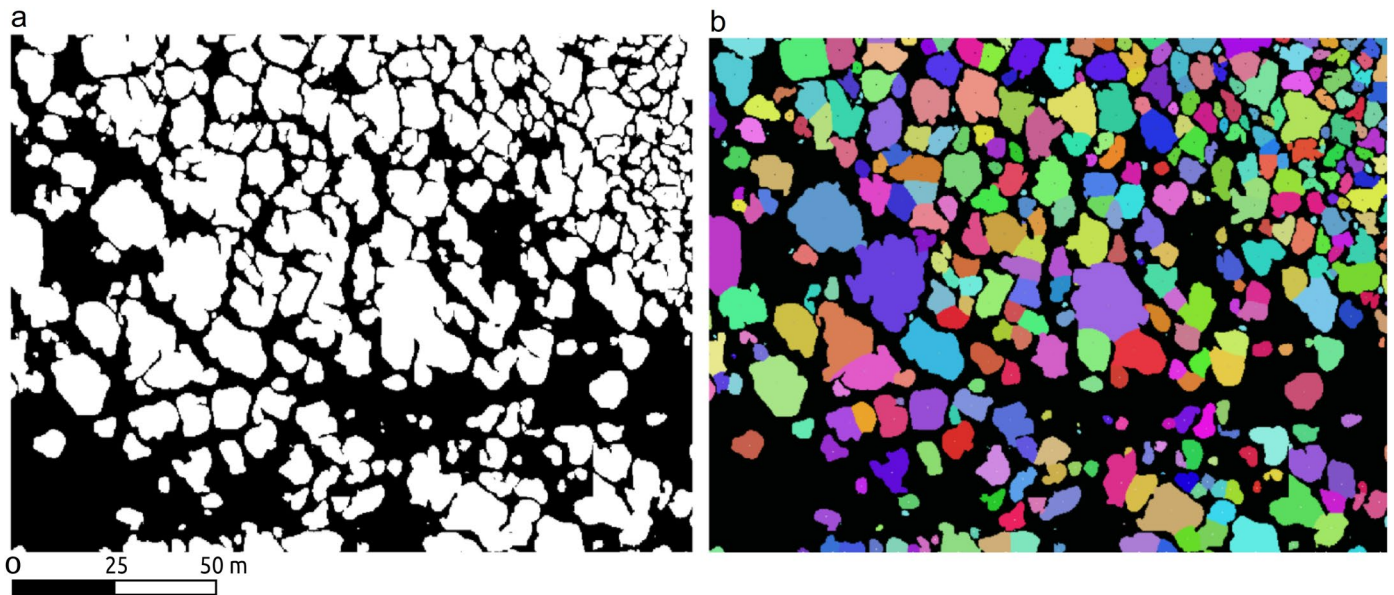
Extended Data Fig. 2 | Examples from the postprocessing algorithm separating clumped trees. a, Example of predicted tree crowns in the rainforest, with many trees being predicted as clumped objects. **b**, Results after the postprocessing algorithm separated the clumped crowns. The algorithm first finds the object centres, and then relabels the image based on weighted distances to the identified centres. Thus, blobs containing multiple centres are divided into various instances accordingly. The algorithm adds a large penalty for not-in-sight centres, and additionally performs a majority filtering to remove the lone-pixels.
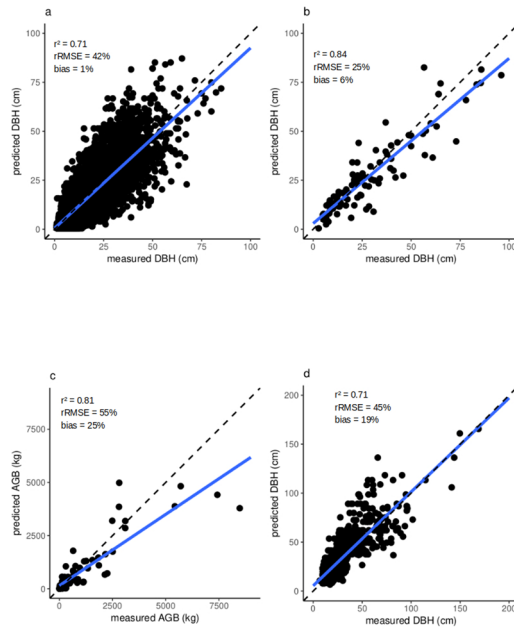
Extended Data Fig. 3 | Tree crown allometry. a, DBH is predicted from CD using a total of 11,593 samples from a global database[36]. The plot compares the predicted against the measured DBH. **b**, DBH is predicted for an independent dataset of 93 trees from Kenya using the equation derived from (a). **c**, We used an allometric equation from literature[37] to calculate AGB from the CD predicted DBH shown in (b). Predicted AGB is here compared with destructively measured AGB. **d**, While samples shown in a–c are all outside forests, (d) shows 793 field-measured trees from Rwanda's natural forest. As in (a), DBH was predicted from CD. The bias was calculated following equation (1).
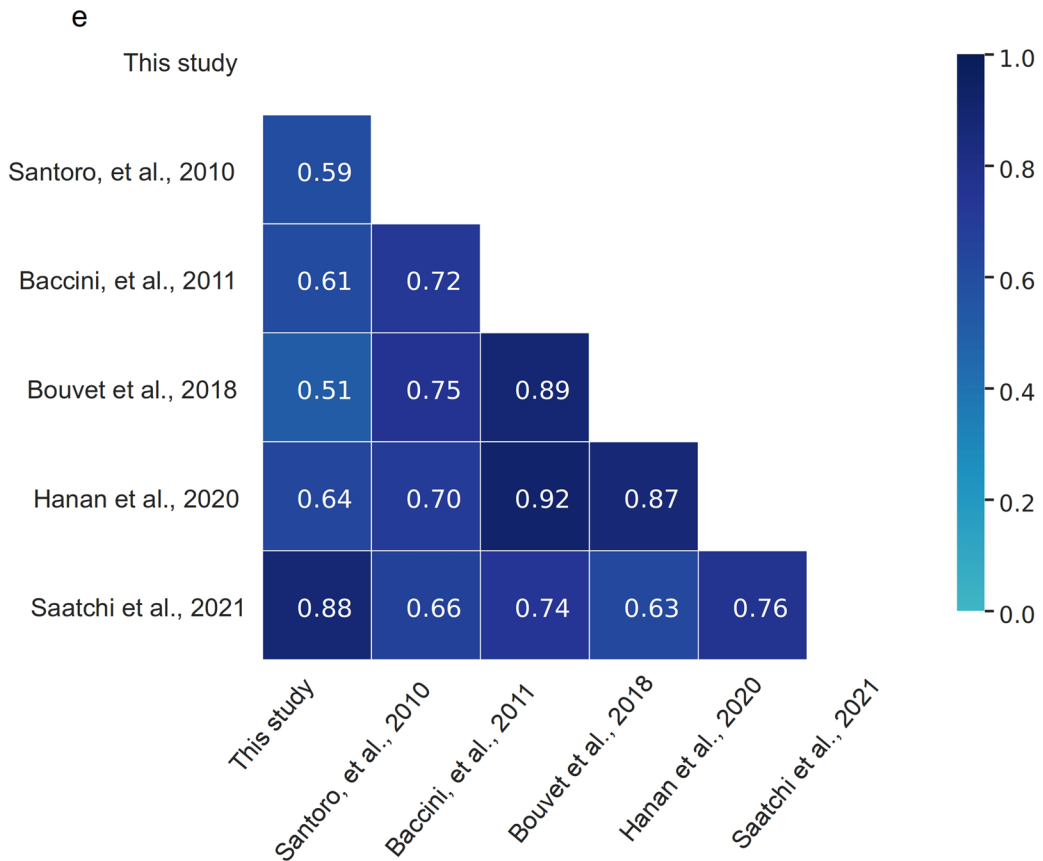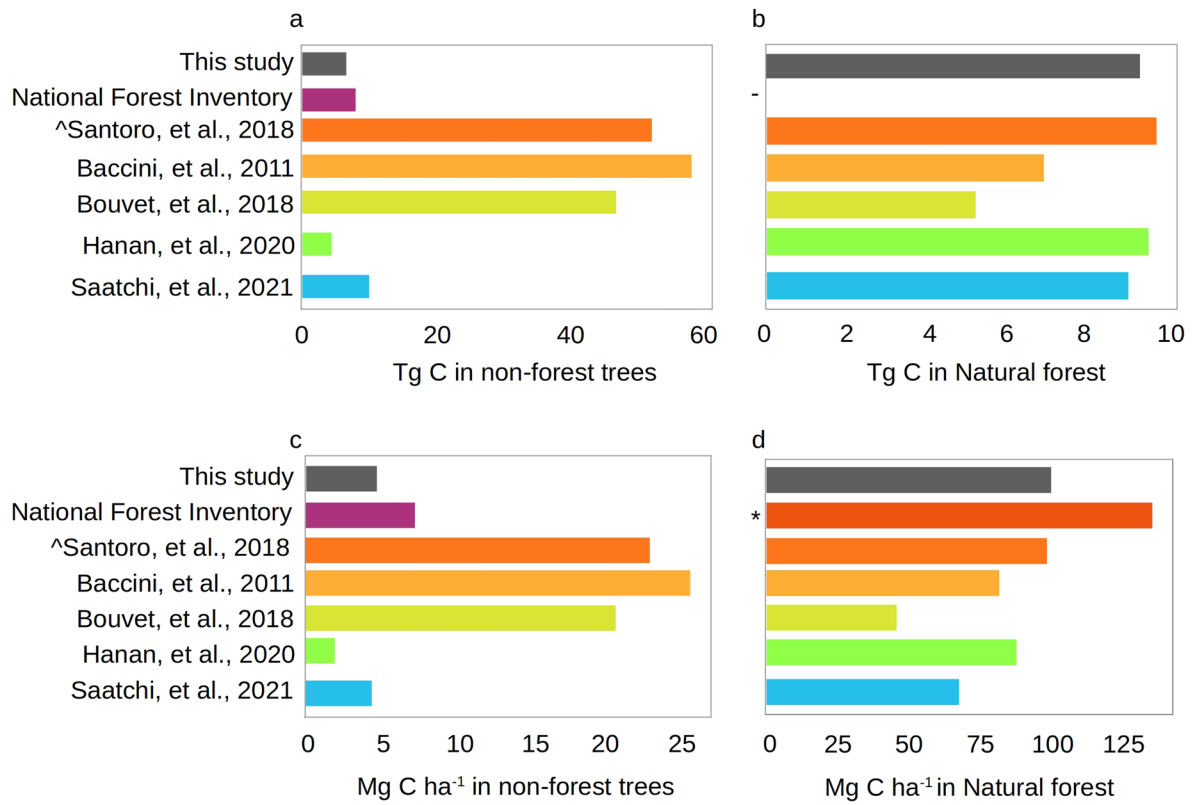
Extended Data Fig. 4 | See next page for caption.

Extended Data Fig. 4 | Comparison of aboveground carbon estimations at country scale. a, Comparison of predicted total aboveground carbon stocks by this study, NFI and existing global products for non-forest areas. **b**, Same as (a) but for natural forests. **c**, Comparison of predicted aboveground carbon density by this study, NFI, and existing global products for non-forest areas. **d**, Same as (c) but for natural forests. **e**, Correlation matrix showing the two-tailored Pearson correlation for 1×1 km[2] grids between different biomass datasets. Note that ref. [45] does not report values above 85 Mg biomass per hectare (Supplementary Fig. 2), explaining the lower correlation values. P < 0.001 for all correlations. (^ We selected the 2010 version; - Natural forest is not considered as part of the NFI; * ref. [40] and ref. [41]).
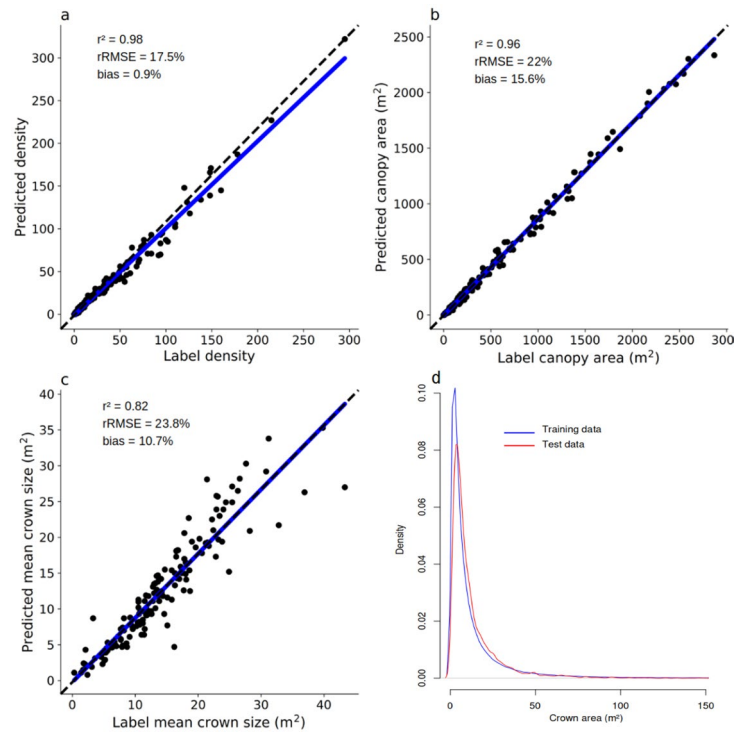
**Extended Data Fig. 5 | Tree crown model evaluation at plot level.** We manually labelled 6,591 trees and compared predictions and labelled trees at plot level. **a**, Tree density, **b**, canopy area, **c**, mean crown size. Each point represents one 25×25 m grid, n = 153. The bias was calculated following equation (2). **d**, Density distribution of the crown areas in the training and test dataset.
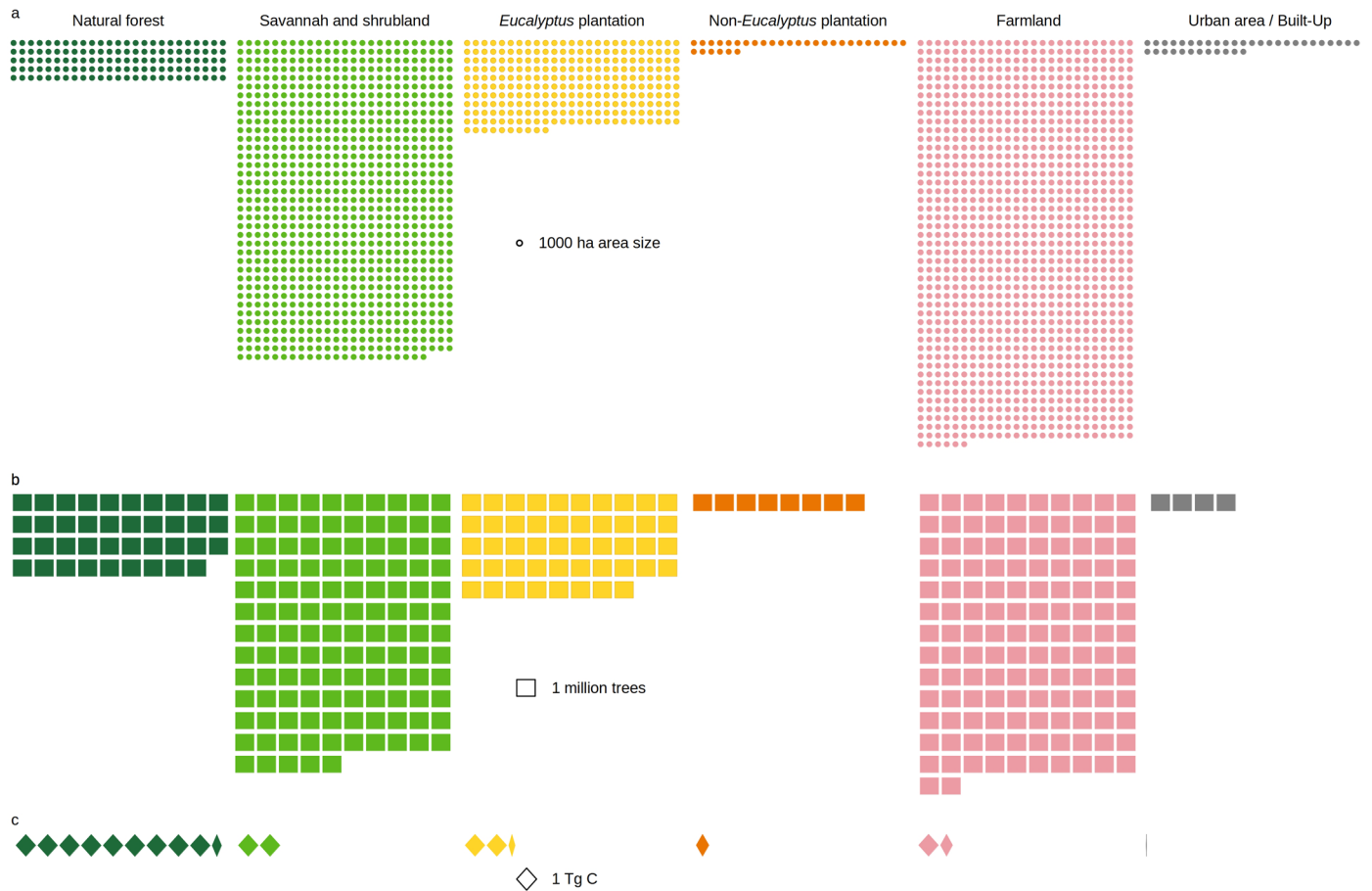
**Extended Data Fig. 6 | Visual illustration of tree count and carbon stock per land cover type in Rwanda. a**, Area size (1000 ha) covered by different land cover types, and **b**, tree count per land cover type (million trees), and **c**, carbon stocks per land cover type (TgC). Although natural forests cover a small portion of land, they are home to a remarkable number of trees with the largest C stocks of the country.
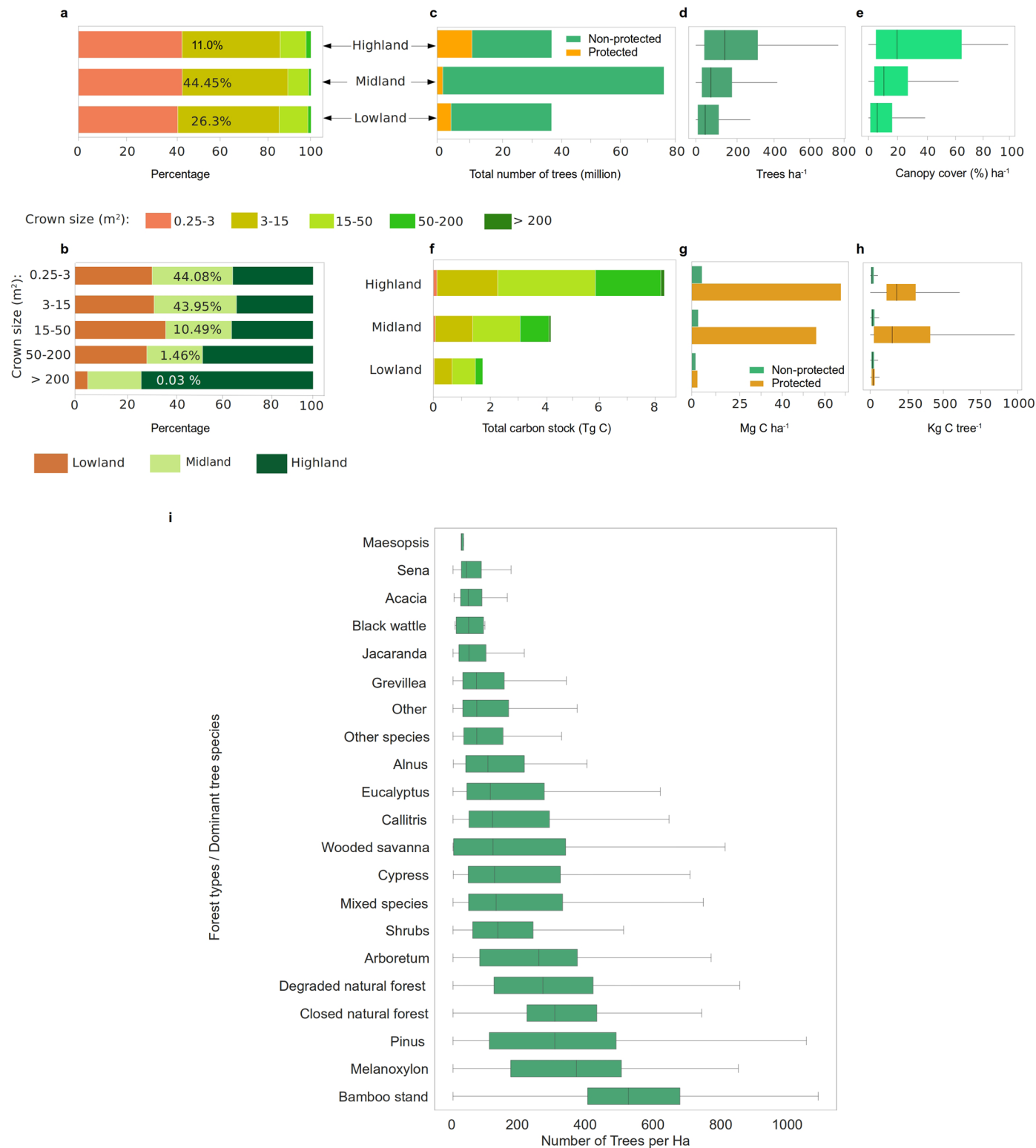
Extended Data Fig. 7 | Tree properties of different landscape types. a,
Percentage covered by different crown sizes in each landscape type. The percent
number shows the contribution of the landscape type to the total area. **b,**
Percentage covered by each landscape type in different crown size categories.
c, Total count of trees by landscape type. **d,** Boxplot showing the average
number of trees per ha by landscape type. **e,** Same as d but for tree cover. **f,** Total
estimated carbon stock per landscape type. **g,** Barplots showing the distribution
of average carbon stock per ha per landscape type, and h, boxplots showing

the average carbon stock per tree per landscape type. **i,** Average tree density
per tree species in Rwanda. Species data are from Rwanda national forest map
of 2012[51]. In boxplots in d, e and h (from left to right), the start of the horizontal
line represents the minimum value, vertical lines represents first quartile,
median and third quartile values respectively, and the end of the horizontal
line represents the maximum value. In i, lines from left to right represent the
minimum, first quartile, median, third quartile and maximum values. Number of
trees = 355,268,345.
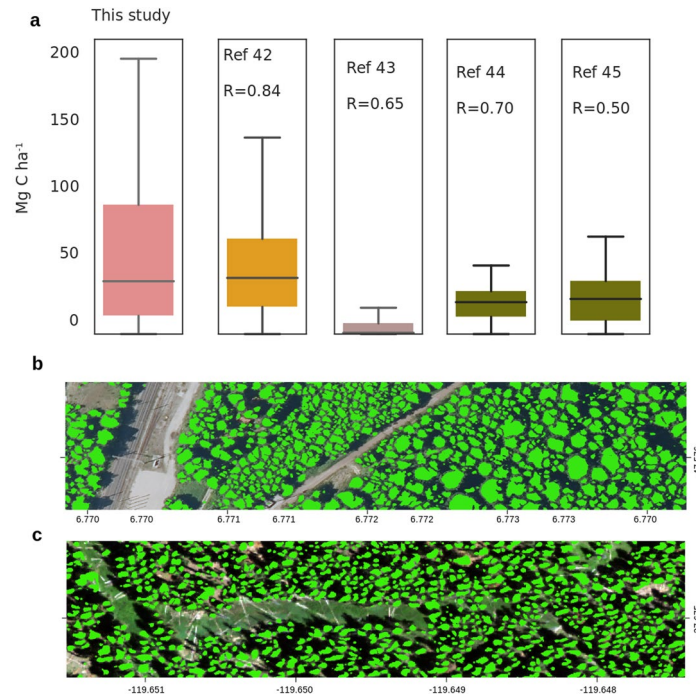
Extended Data Fig. 8 | Beyond Rwanda. a, We took 150 (n = 150) random 1 × 1 km samples and aggregated the predicted tree-level carbon stocks and compared the results to previously published maps using two-tailored Pearson correlation. We did not include ref. [61] because of the coarse native resolution which did not guarantee that the same areas were compared. Note that ref. [45] does not report values above 85 Mg biomass per hectare, explaining the lower correlation values. P < 0.001 for all correlations. **b**, The model trained on the Rwanda aerial images was directly applied on aerial images from France (20 cm) and c, NAIP aerial images at 60 cm. In boxplots in a, lines from top to bottom represent the maximum, third quartile, median, first quartile and minimum values. Credit: photographs in **b**, USGS NAIP; **c**, IGN France.

Extended Data Table 1 | Evaluation with field data

a

	Field data (Mg C ha⁻¹)	This study (Mg C ha⁻¹)	bias (%)	Plots (n)	Source	Relative area at national scale
Plantations	16.8	8.2	52.6	106	NFI*	12%
Savanna and shrubland	3.3	4.2	18.9	116	NFI*	33%
Farmland	2.4	2.5	5.9	150	NFI*	48%
Natural forest	121	81	plots: 11%; sum: 26%	15	*ref 40 and ref 41*	5%

b

Uncertainty source	Method	Evaluation	Forest	Non-Forest	Level
Tree count	Manual expert labels	Independent test data	error = 13%	error = 2.9%	Biome
Canopy area	Aggregate tree crowns	Independent test data	Crown area*0.27 to correct for gaps; bias = 13%	error = 14.9%	Biome
Crown diameter to DBH conversion	Allometry	4 equations each using 50% of the field data	error = 19%	error = 6%	Tree
Error propagation from allometry	Allometry	Prediction of each tree in Rwanda with 4 different equations	error = 2.3%	error = 3.9-6.2% (varies with land cover)	Biome
Wood density	Fixed at 0.54	ref 40, ref 64	error = 18.2%	error = 25% (n = 1985)	Tree
DBH to AGB	Allometry	ref 36; ref 37	error = 9.7%	error = 2.5%	Tree
AGB to AGC	Fixed factor of 0.47	ref 56	varies, highest error = 8.9%	-	Tree
Overall predicted crown area to AGB	**See above**	**373 NFI permanent plots, 15 forest plots**	**error = 26%**	**error = 16%**	**Biome**

a, We compared our tree-level carbon stock estimates aggregated to 1ha grids with field data from different sources. The exact location of the NFI plots was unknown, so we used averages of the areas close by. The statistics were then calculated for averages per class, except for natural forests where exact plot coordinates were available, therefore, comparisons could be done per plot. We then weighted the bias according to the relative area at the national scale to derive a nation-wide uncertainty of 16.9% (NFI total C in TOF: 8.35 TgC; this study estimates 6.95 TgC). *The NFI original measurements are the aboveground biomass expressed in volume (m³). We have converted them in weight (metric tonnes) using the conversion rate: 1 m³=0.714 tonne (ref. [65]) which assumes an overall average wood density of 0.714 g/cm³ per tree, then multiplied by the AGB-to-AGC conversion factor: 0.47 to get the C equivalent. b, Different sources of uncertainty and how we evaluated and quantified their impact. Errors at the biome level may be systematic. Errors at tree level were evaluated with equation (1), and errors at biome and plot level with equation (2)

Extended Data Table 2 | Evaluation

a

	RMSE in Mg C/ha (rRMSE)	Bias (%)
Farmland	0.08 (5%)	5.9
Savanna and shrubland	0.1 (5%)	5.1
Plantations (Eucalyptus)	0.2 (2%)	6.2
Plantations (non-Eucalyptus)	0.4 (2%)	3.9
Natural forest	1.7 (2%)	2.3

b

All:

	Tree detected	No tree detected
Tree label exists	TP = 80%	FN = 20%
No tree label	FP = 7%	TN = 99%

Forest:

	Tree detected	No tree detected
Tree label exists	TP = 81%	FN = 18%
No tree label	FP = 7%	TN = 97%

Non-forest:

	Tree detected	No tree detected
Tree label exists	TP = 79%	FN = 20%
No tree label	FP = 6%	TN = 99%

a, Evaluation of the crown diameter to stem diameter conversion. Four CD–DBH equations were established, each using a random subset of 50% of the data. Tree biomass was predicted with each equation and aggregated to the hectare level. We then calculated the RMSE, rRMSE and bias between the 4 predictions for each 1 ha grid. Results shown here are aggregated over land cover classes. b, Tree crown model evaluation at pixel level. Confusion matrix between predicted and 6,591 manually labelled trees. These data are independent and were not used to establish or validate the model and the results.

nature research

Corresponding author(s): Martin Brandt; Maurice Mugabowindekwe

Last updated by author(s): Oct 20, 2022

Reporting Summary

Nature Research wishes to improve the reproducibility of the work that we publish. This form provides structure for consistency and transparency in reporting. For further information on Nature Research policies, see our Editorial Policies and the Editorial Policy Checklist.

Statistics

For all statistical analyses, confirm that the following items are present in the figure legend, table legend, main text, or Methods section.

n/a	Confirmed	
☐	☒	The exact sample size (n) for each experimental group/condition, given as a discrete number and unit of measurement
☒	☐	A statement on whether measurements were taken from distinct samples or whether the same sample was measured repeatedly
☐	☒	The statistical test(s) used AND whether they are one- or two-sided *Only common tests should be described solely by name; describe more complex techniques in the Methods section.*
☒	☐	A description of all covariates tested
☒	☐	A description of any assumptions or corrections, such as tests of normality and adjustment for multiple comparisons
☐	☒	A full description of the statistical parameters including central tendency (e.g. means) or other basic estimates (e.g. regression coefficient) AND variation (e.g. standard deviation) or associated estimates of uncertainty (e.g. confidence intervals)
☒	☐	For null hypothesis testing, the test statistic (e.g. F, t, r) with confidence intervals, effect sizes, degrees of freedom and P value noted *Give P values as exact values whenever suitable.*
☒	☐	For Bayesian analysis, information on the choice of priors and Markov chain Monte Carlo settings
☒	☐	For hierarchical and complex designs, identification of the appropriate level for tests and full reporting of outcomes
☒	☐	Estimates of effect sizes (e.g. Cohen's d, Pearson's r), indicating how they were calculated

Our web collection on statistics for biologists contains articles on many of the points above.

Software and code

Policy information about availability of computer code

Data collection	The aerial image data were provided by the Centre for Geographic Information Systems and Remote Sensing of University of Rwanda. There was no special software involved
Data analysis	Only free and open source software was used for data analysis: Python (3.8), RStudio (1.4), QGIS (3.22), GDAL tools (3.1). The deep learning code was written in Python (3.8) using Tensoflow (2.5). The clumped trees separation code was written in Python (3.8)

For manuscripts utilizing custom algorithms or software that are central to the research but not yet described in published literature, software must be made available to editors and reviewers. We strongly encourage code deposition in a community repository (e.g. GitHub). See the Nature Research guidelines for submitting code & software for further information.

Data

Policy information about availability of data

All manuscripts must include a data availability statement. This statement should provide the following information, where applicable:

- Accession codes, unique identifiers, or web links for publicly available datasets
- A list of figures that have associated raw data
- A description of any restrictions on data availability

Global tree cover maps are available at http://earthenginepartners.appspot.com/science-2013-global-forest. Climate data are freely accessible through an online application to the Rwanda Meteorological Agency via http://mis.meteorwanda.gov.rw/. Aerial images, and land use and land cover data are freely available for research through formal application to the Rwanda Land Management and Use Authority: https://www.rlma.rw. Products produced in this study: tree density, tree cover, carbon stock estimates are freely accessible at https://doi.org/10.5281/zenodo.7118176 (ref 65). The global database with tree measurements including biomass is available from J.C.. Tree measurements from Kenya are available from D.S.. Tree measurements from Rwanda are available from M.M.. Any more relevant data can be availed upon reasonable request addressed to the corresponding authors.

Field-specific reporting

Please select the one below that is the best fit for your research. If you are not sure, read the appropriate sections before making your selection.

☐ Life sciences   ☐ Behavioural & social sciences   ☒ Ecological, evolutionary & environmental sciences

For a reference copy of the document with all sections, see nature.com/documents/nr-reporting-summary-flat.pdf

Ecological, evolutionary & environmental sciences study design

All studies must disclose on these points even when the disclosure is negative.

Study description	This study uses 198 aerial images at 0.25 m2 resolution. We used a deep learning algorithm trained on 97,574 hand-lebelled tree crowns to map 355,268,345 trees with a crown size larger than 0.25 square meters both inside and outside forests in Rwanda, a country located in East Africa, spanning a wide range of African landscapes: natural forests including tropical montane rainforest, savannas, shrublands, tree plantations including young plantations and coppices, agroforestry trees in farmlands, and isolated trees. Furthermore, we apply state-of-the art allometric equations to estimate and map carbon stock of every mapped individual tree at the national scale.
Research sample	The study is a nation-wide mapping of individual tree carbon stocks, where over 355 million trees were mapped, and charecterised in terms of their crown size and carbon stock all over Rwanda: a country with surface area of more than 25 thousand square kilomeres, excluding an area of about 4,000 square kilometers where 0.25 m resolution aerial images were not available.
Sampling strategy	We did not do a specific sampling, because all trees and shrubs are included in the study. However, we have excluded any woody plant with a crown size below 0.25 m2, a threshold set based on the visual inspection of the aerial images, as trees of this size and above were still clearly visible
Data collection	We use publicly available aerial images of Rwanda at 0.25x0.25 m resolution, collected in June - August of 2008 and 2009. The images were acquired from 3000 meter altitude above ground level, initially with a mean ground resolution of 0.22x0.22 m pixel size, using a Vexcel UltraCam-X aerial digital photography camera. They include a red, green, and blue band stored under 8 bit unsigned integer format. The aerial images cover 96% of the country, and the remaining 4% was filled by satellite images from WorldView-2, Ikonos, Spot, and QuickBird satellite sensors which are part of the publicly available dataset. For the carbon stocks estimation, we conducted a field campaign in December 2021 and measured 793 trees in the natural forest, and also used previously published 10,591 measurements of pan-tropical non-forest trees, as well as previously published 952 non forest trees from Kenya. We validated the results with data from the Rwanda National Forest Inventory (NFI) from 2013/2014 collected in 373 NFI permanent plots with 2,415 trees, and previously published 6161 measurements of afromontane rainforests in Rwanda.
Timing and spatial scale	The aerial images are from June-August 2008 and 2009, and cover the extent: 28.86,-2.84 : 30.90,-1.05 of Rwanda in East Africa.
Data exclusions	Aerial images were taken only during dry season of 2008 and 2009 because it is time when the sky is clear and features on the ground are very visible for the air-borne or space-borne sensor. However, 4% of the country (about 100,000 km2) was not covered by the aerial images due to permanent clouds or trans-boundary security issues during the images acquisition, which made it imperative to opt for image fusion approach using WorldView-2, Ikonos, Spot, and QuickBird satellite images. However, there is an area about 4,000 km2 around the location (longitude: 29.62, latitude: -1.95) where fusion has used a 2.5-m resolution images from Spot satellite sensor, and trees were not accurately visible. This area was excluded from further analysis.
Reproducibility	Data were processed 3 times at different time intervals leading to the same results
Randomization	NA, we have used all 355 milllion trees with no sampling
Blinding	NA, we have used all 355 million trees with no sampling
Did the study involve field work?	☒ Yes ☐ No

Field work, collection and transport

Field conditions	Fieldwork was conducted in December 2021. The conditions were humid with temperatures around 20oC
Location	The data collection was done in South-western part of Rwanda, in the tropical montane forest located in a protected area of Nyungwe National Park (29.31, -2.51)
Access & import/export	NA, the data were noted digitally
Disturbance	Measuring the tree dimensions (crown diameter, tree height, diameter at breast height, tree location) did not involve disturbances. However, since the field collection area is a protected area with a natural forest, we had to work with forest rangers to guide our field work and advise on accessible plot locations. This way, we followed existing trails and ensured not to do any destructive sampling or vegetation clearing for new trails. To abide by the conditions of the area, our sample plots were limited to locations within 200 m from the existing major roads within the forest

Reporting for specific materials, systems and methods

We require information from authors about some types of materials, experimental systems and methods used in many studies. Here, indicate whether each material, system or method listed is relevant to your study. If you are not sure if a list item applies to your research, read the appropriate section before selecting a response.

Materials & experimental systems		Methods	
n/a	Involved in the study	n/a	Involved in the study
☒ ☐	Antibodies	☒ ☐	ChIP-seq
☒ ☐	Eukaryotic cell lines	☒ ☐	Flow cytometry
☒ ☐	Palaeontology and archaeology	☒ ☐	MRI-based neuroimaging
☒ ☐	Animals and other organisms		
☒ ☐	Human research participants		
☒ ☐	Clinical data		
☒ ☐	Dual use research of concern		